

Ondes stationnaires combinées à l'émission X ou à la photoémission X pour l'étude de films minces



Philippe JONNARD

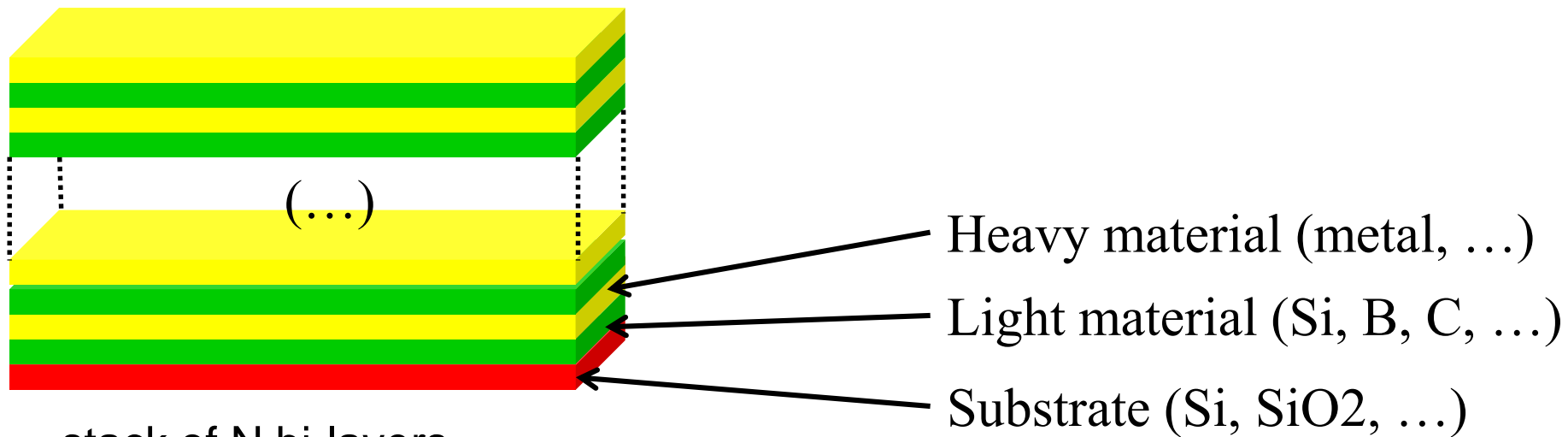


*Laboratoire de Chimie Physique –
Matière et Rayonnement
Sorbonne Université, CNRS UMR 7614, Paris*

Séminaire de l'Institut des Matériaux Jean Rouxel, Nantes, 4 avril 2019

Periodic multilayers for EUV and X-ray ranges

Extreme UV : 20 – 200 eV 0.6 – 6 nm
Soft x-ray : 200 – 5000 eV 0.25 – 0.6 nm



stack of N bi-layers

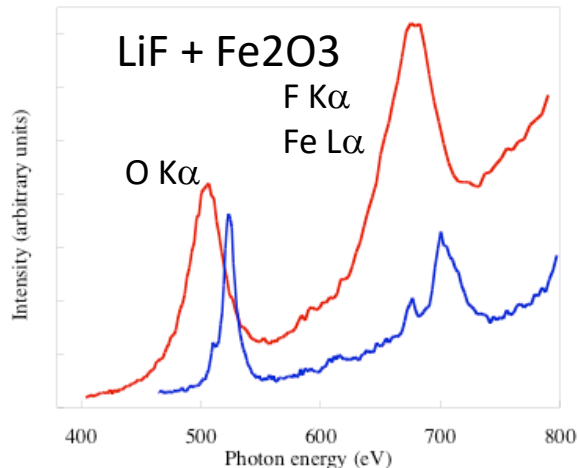
thickness_{light} + thickness_{heavy} = period d of a few nm

↳ can diffract EUV and x-rays

$$\text{Bragg law : } p\lambda = 2d \sin\theta$$

Applications of multilayers

- Solar images from spatial telescopes
- Photolithography @ 13.5 nm
- Optical components for synchrotron beamlines
- Optical components for new x-ray sources (x-ray laser, high harmonic generation, ...)
- Optics for diffraction apparatus



X-ray emission spectroscopy

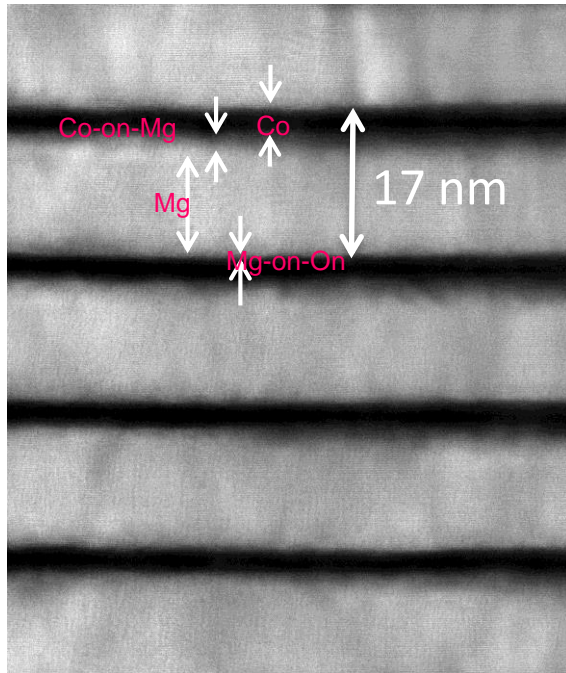


Imaging at a given wavelength

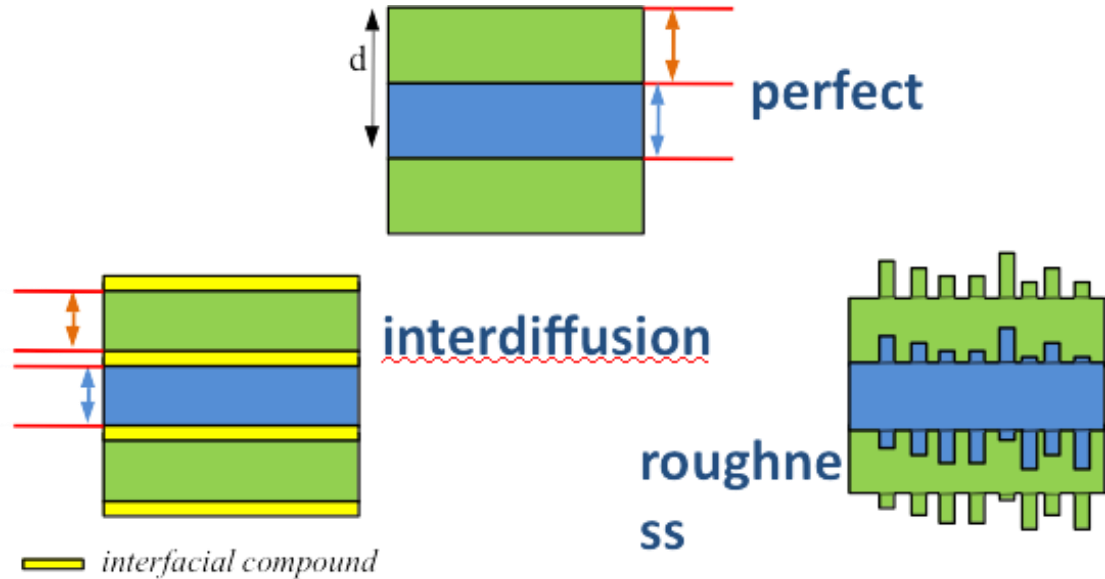


Photolithography
@ 13.5 nm, 6.x nm

Motivation and challenges



Co
Mg
Co
Mg
Co
Mg

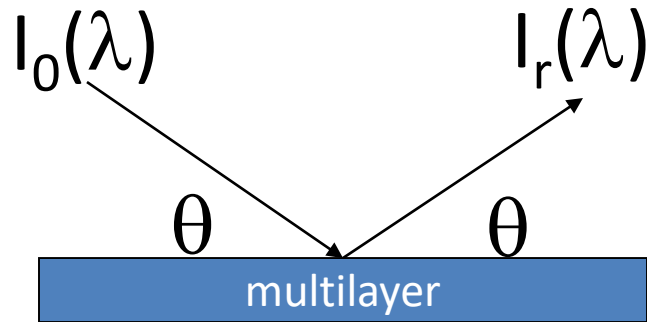


	Visible $\lambda=500\text{nm}$	EUV $\lambda=30.4\text{nm}$
d	$\sim 125\text{nm}$	Co_2.6nm/Mg_13.6nm
σ	$\sim 10\text{ nm}$	$\sim 0.5\text{-}0.8\text{nm}$

R multiplied by **DW factor**
 $\exp(-2[2\pi\sigma \sin\theta / \lambda]^2)$
 $\exp(-2[\pi \sigma/d]^2)$

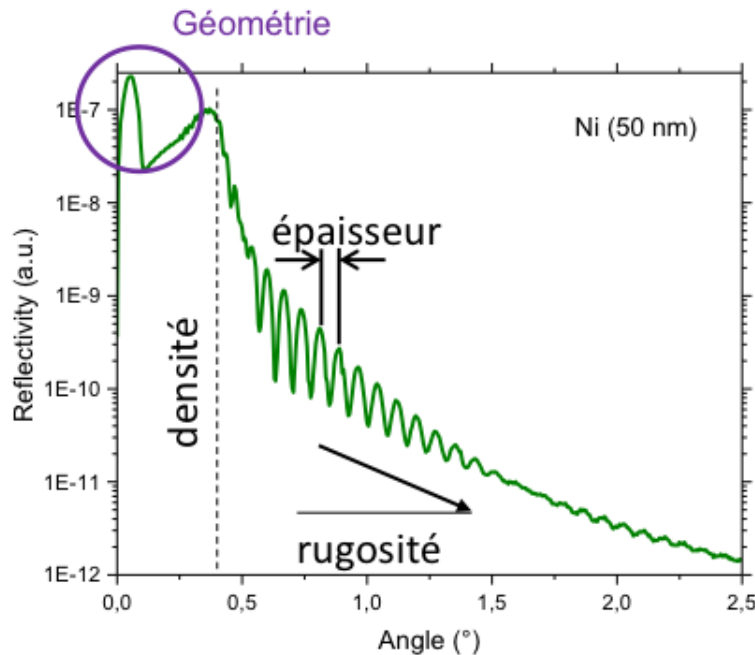
Interface is the largest challenge for EUV multilayer!

X-ray reflectivity



$$R(\theta) = I_r(\lambda) / I_0(\lambda)$$

$$R(\lambda) = I_r(\theta) / I_0(\theta)$$



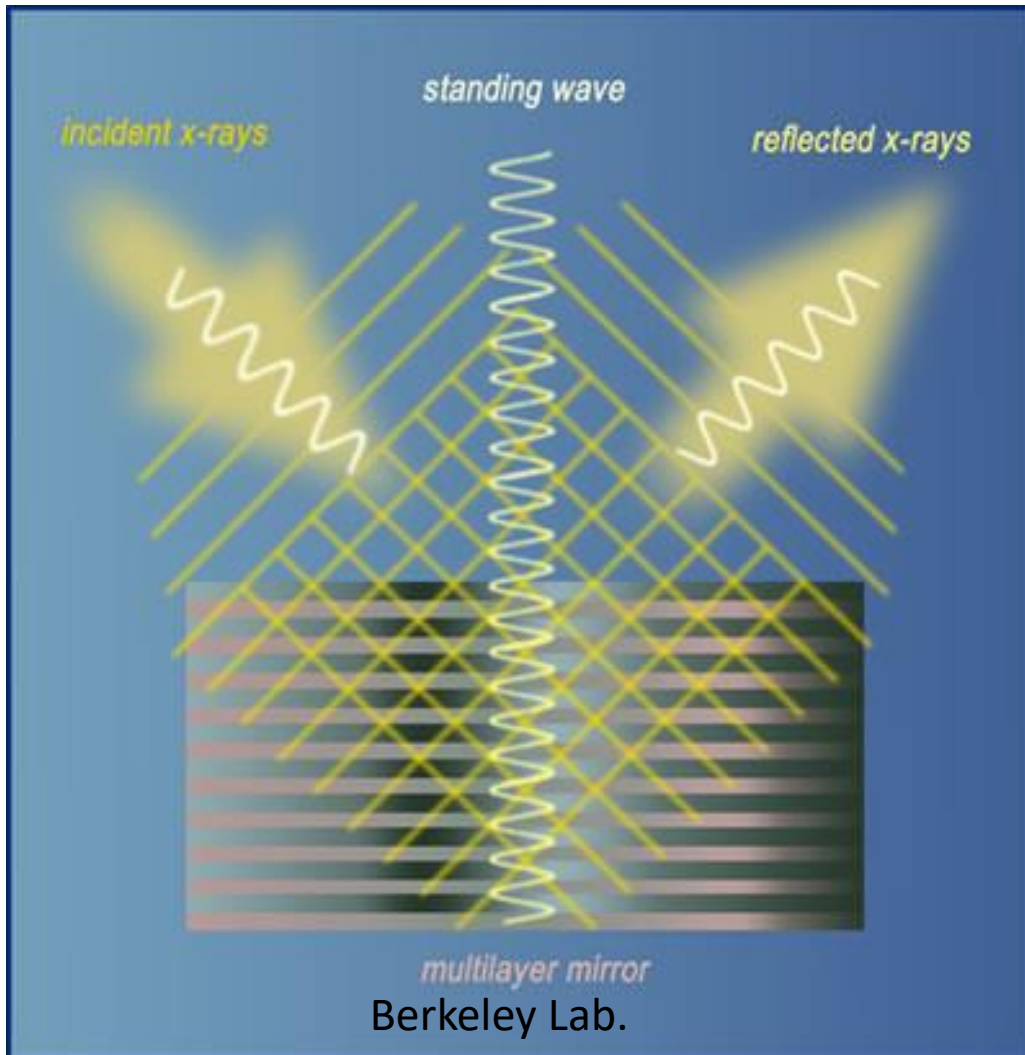
Determination of parameters
of the stack

- thickness
- roughness
- density / optical index
of the various layers

- Les ondes stationnaires (XSW)
- XSW – XRF: Co/Mg/Zr
- XSW – HAXPES: Pd/Y/B4C
- Kossel – XRF: Pd/Y/B4C

- Les ondes stationnaires (XSW)
- XSW – XRF: Co/Mg/Zr
- XSW – HAXPES: Pd/Y/B4C
- Kossel – XRF: Pd/Y/B4C

X-ray standing waves



Generally used

- In **hard** x-ray range
- In **glancing incidence**
- With crystal or
- With multilayer (set of **bilayers**)

To probe

- thin layer on **top of the multilayer**
- **Interfaces of the multilayer** itself

By using

- Fluorescence or photoelectrons

In (or close to) **Bragg conditions**

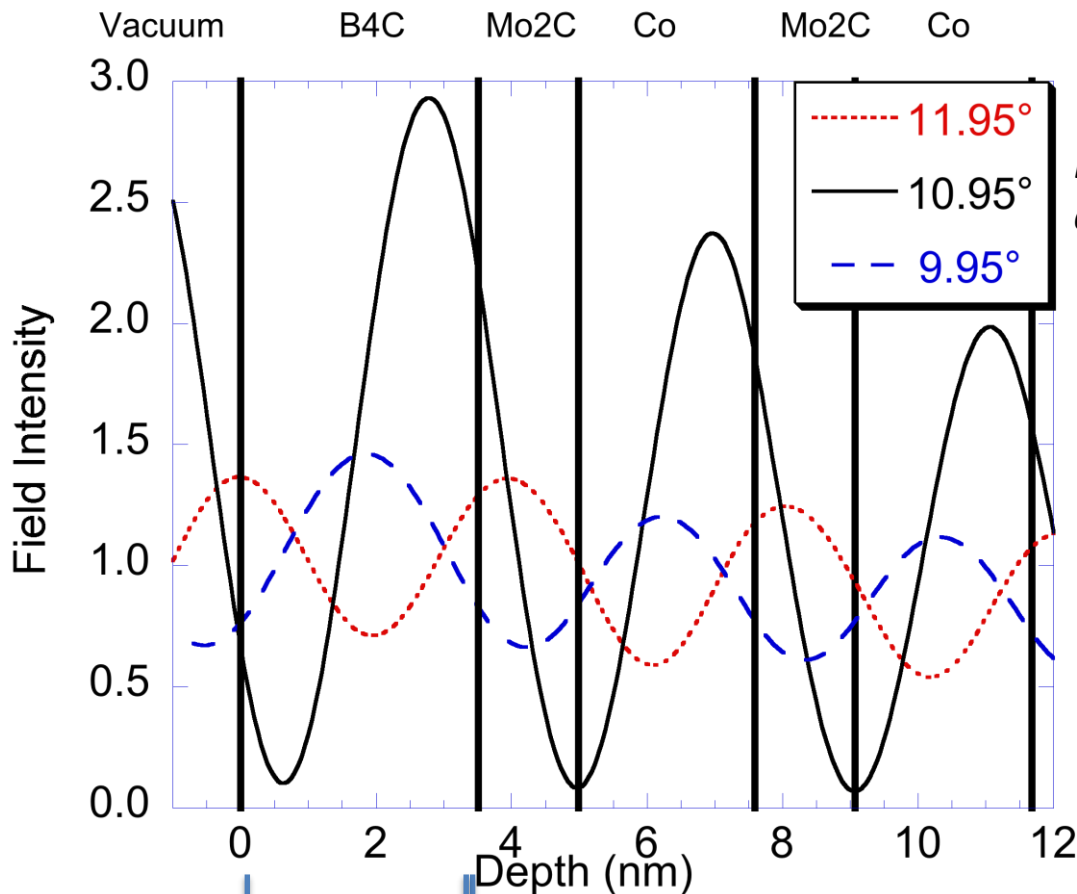
- a strong standing wave develops inside and outside the multilayer
- having the period of the multilayer

X-ray standing waves

Depth distribution of the electric field

Co/Mo2C $d = 4$ nm

$E = 780$ eV (1.6 nm)



Bragg angle

Rotate sample

(change the wavelength)

Change incident or detection angle

Shift of the nodes and anti-nodes

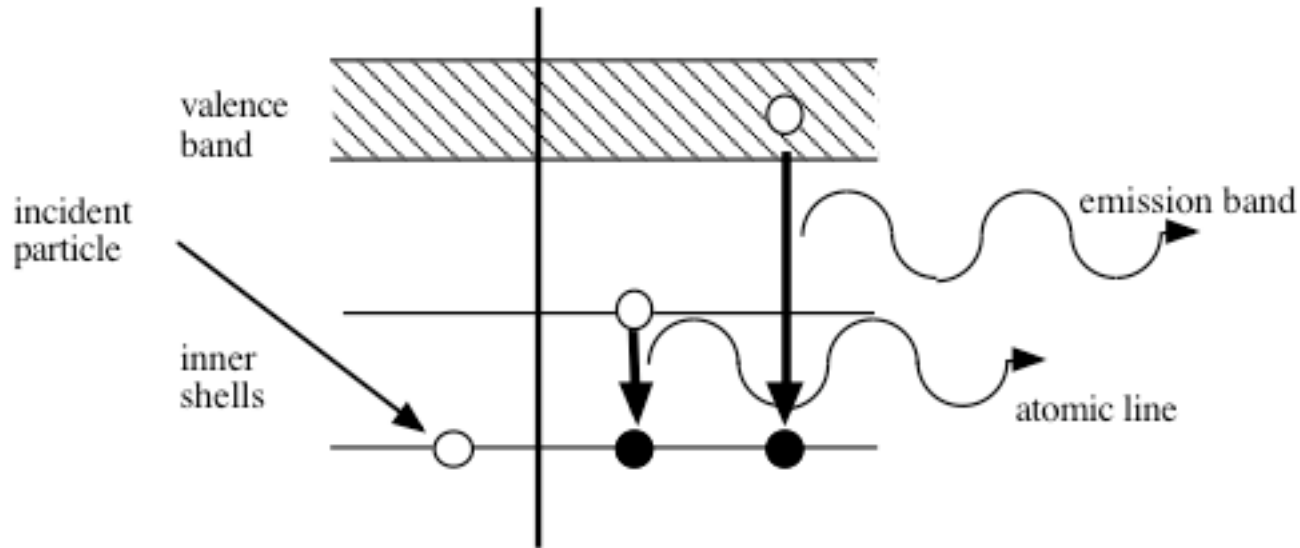
Analysis by **XPS**

XRF

AES

of a **Multilayer**
Superficial material

X-ray emission spectroscopy



Observation of the energy distribution of the emitted radiation
Information about the **chemical state of the emitting element**

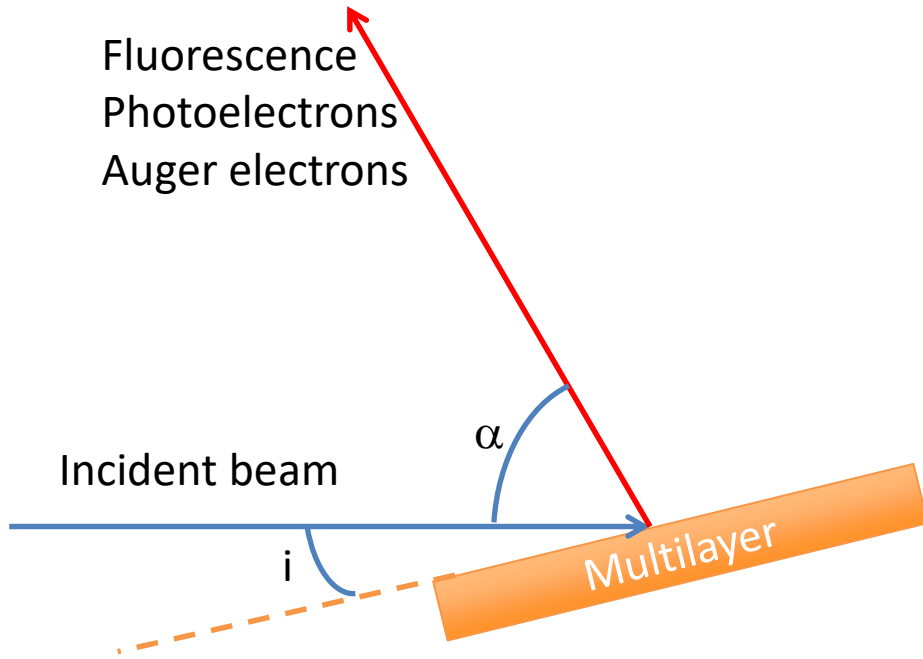
Incoming beam

- **Electrons**
- **Particles**
- **X-rays**

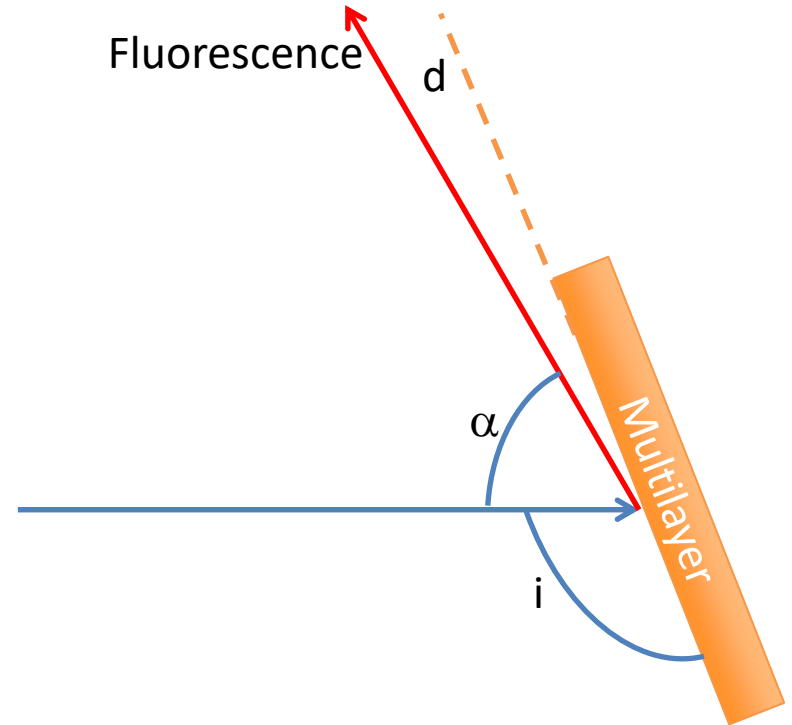
Detection / dispersion

- **WDS : crystal spectrometer**
- **EDS : Si(Li), SDD, bolometer
energy dispersive CCD camera**

Two XSW modes

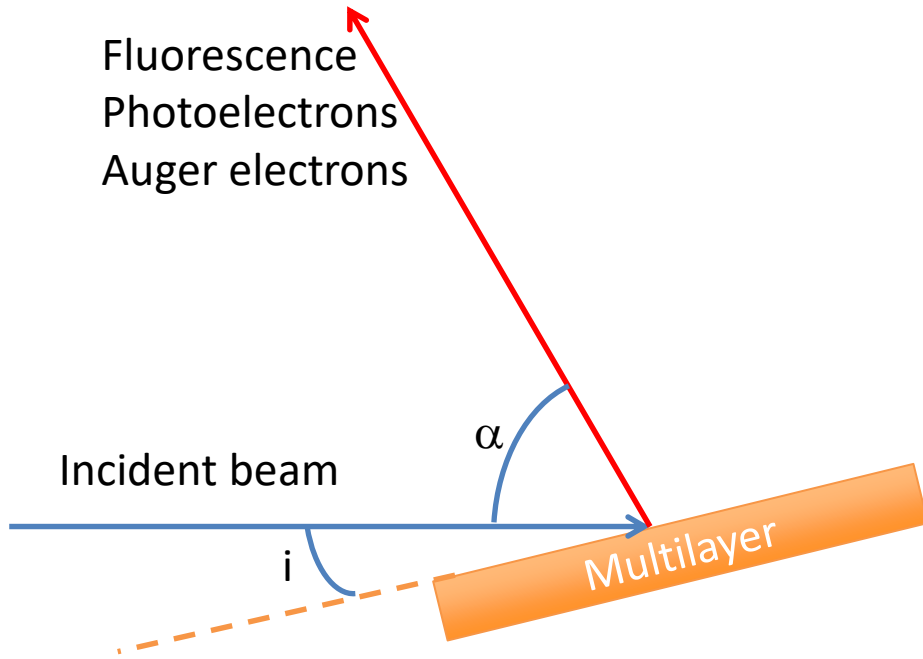


Glancing incidence mode
“Standard” or GI



Glancing exit mode
“Kossel” or GE

Two XSW modes



Incident beam = x-ray beam

Requires synchrotron

x-ray tube

Geometry to be fulfilled

Generally very grazing

Detected beam

No special geometry requirement

Large solid angle of detection possible

Glancing incidence mode

“Standard” or GI

Two XSW modes

Incident beam = any ionizing beam

X-rays

Electrons

Ions

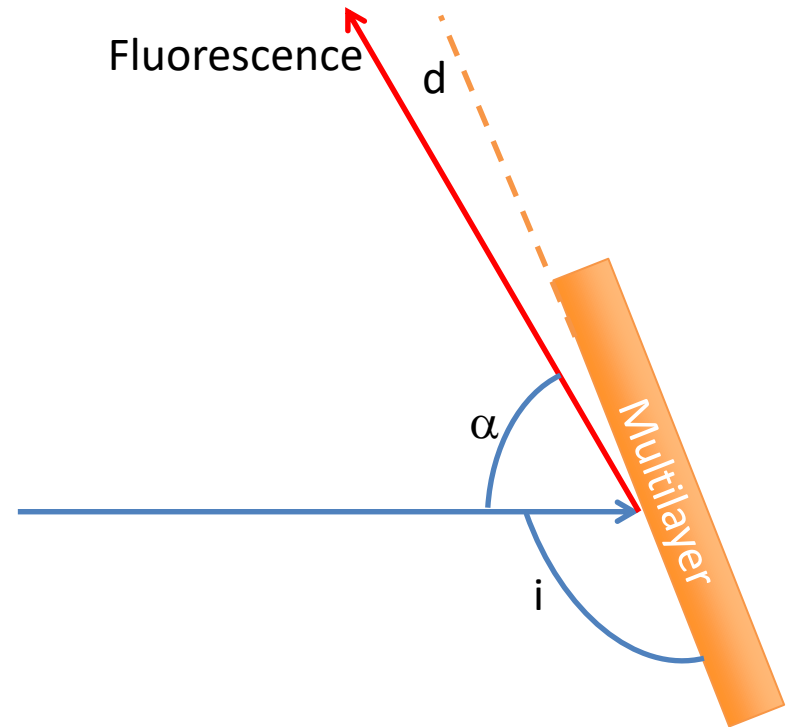
No geometry requirement

**Detected beam =
characteristic x-rays**

Geometry requirement

Generally very grazing

Small solid angle of detection



Glancing exit mode

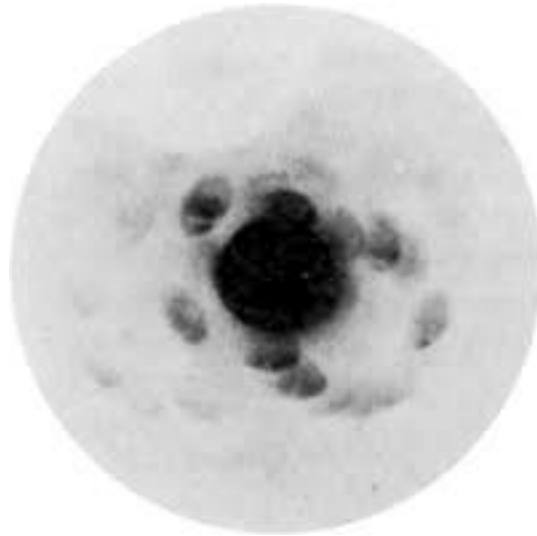
“Kossel” or GE

A bit of history



M. Von Laue

Nobel prize 1914 for his discovery of the x-ray diffraction by crystals



First x-ray diffraction pattern

Hydrated copper sulfate

P1 triclinic

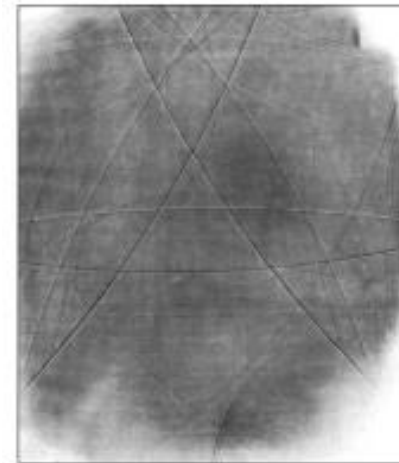
1912: von Laue, Friedrich, Knipping



W. Kossel

1935

Diffraction of the fluorescence produced within the crystal by the crystal itself



Multilayer

Si substrate /

[Mg (5.1nm) / Co (2.6nm)]x30 /

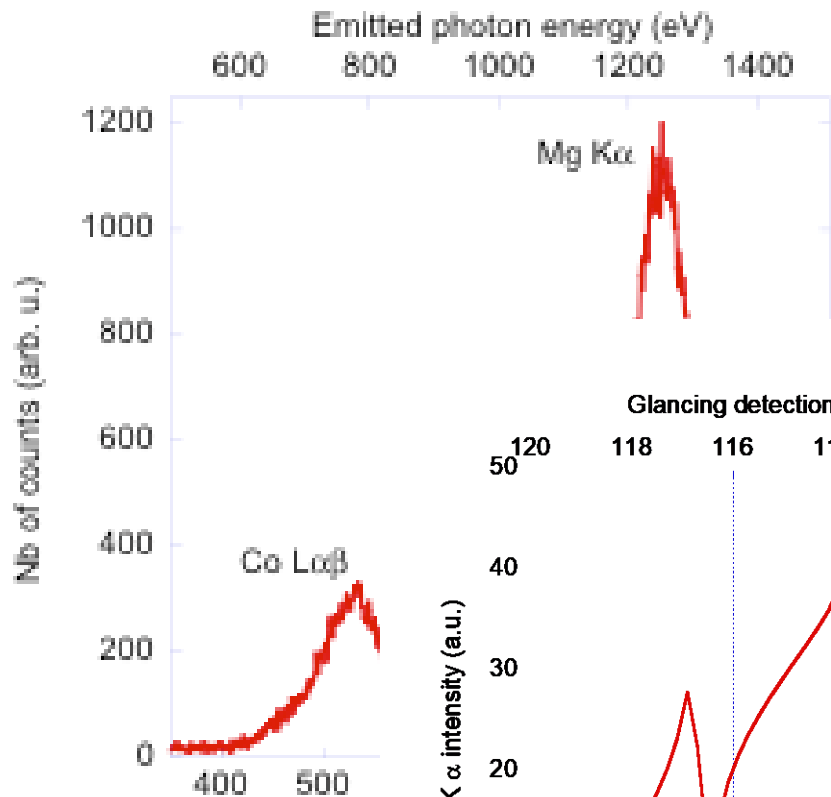
B4C (3.5nm) capping layer

Mg/Co XSW - XRF

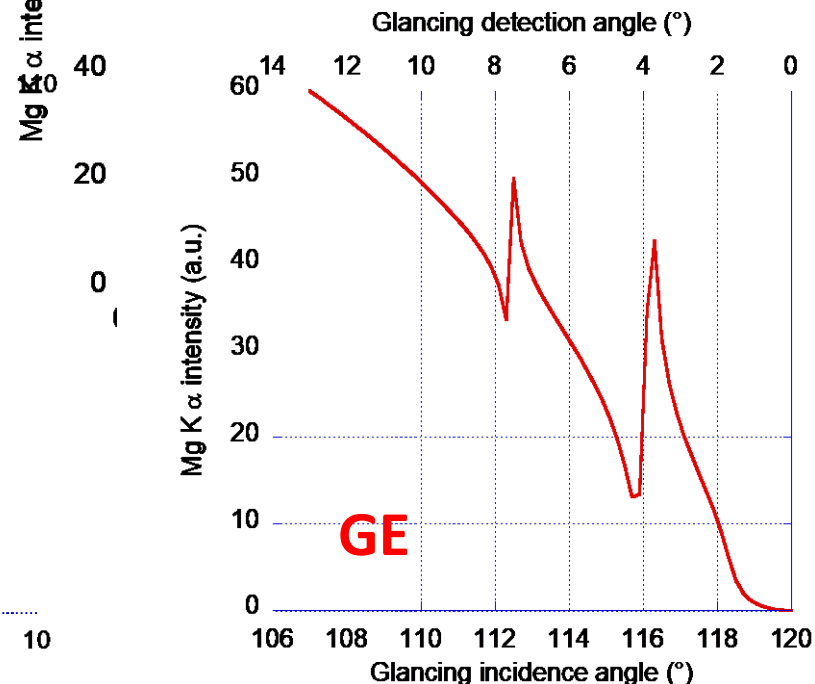
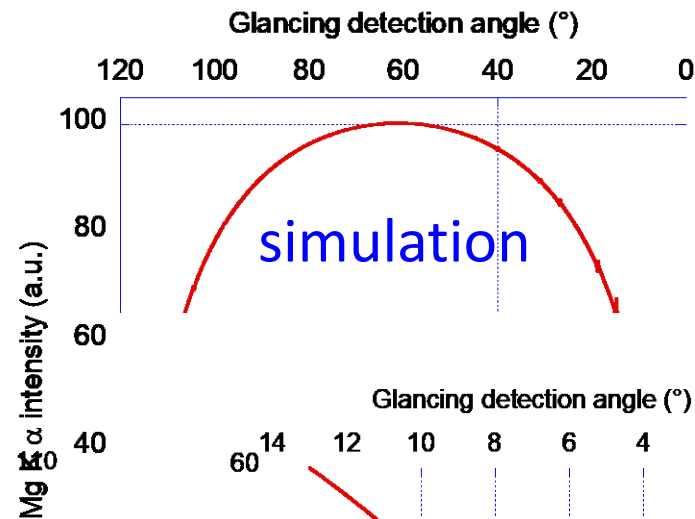
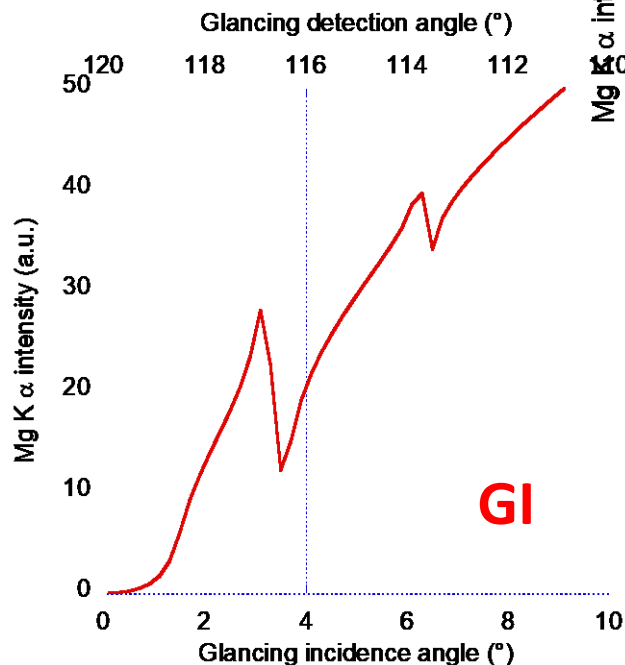
Incident radiation 1500eV; 0.827nm

Mg K α emission 1253.6eV; 0.989nm

60° between incident and detection directions



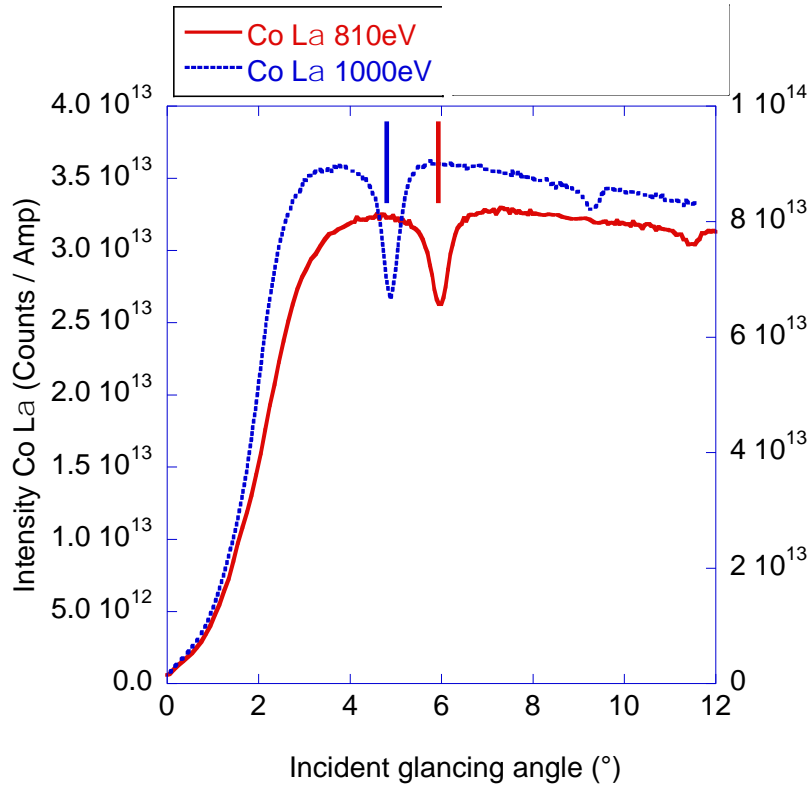
X-ray em



Fluorescence of Mg/Co multilayer

Si substrate / [Mg (5.1nm) / Co (2.6nm)]x30 / B4C (3.5nm)

"Classic" - GIF mode

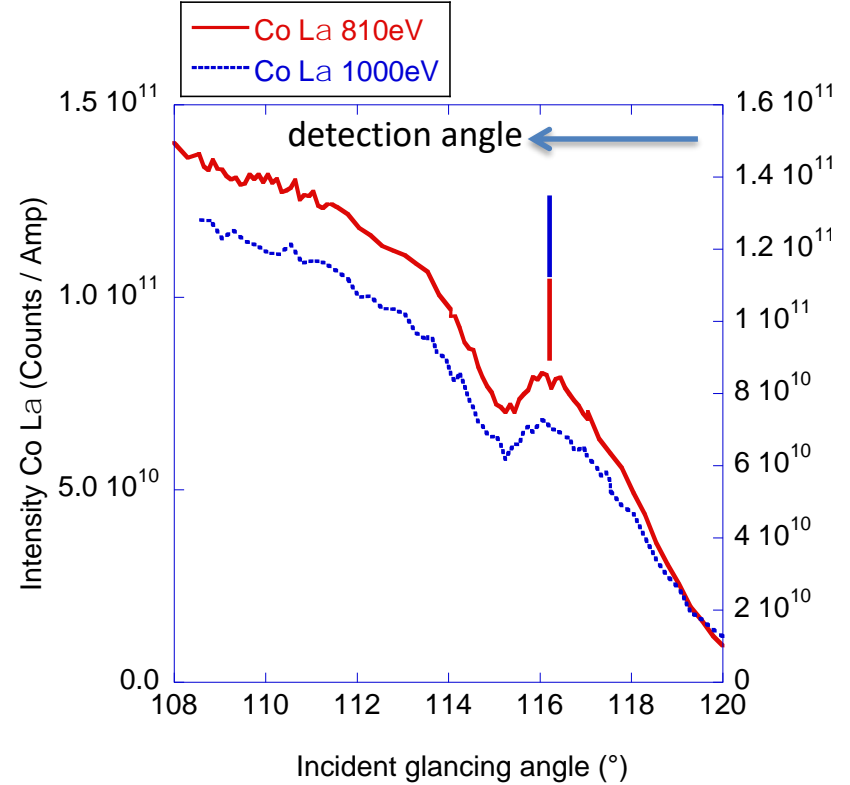


Features appear at Bragg angle of **incident** radiation



Move with energy of incident radiation

"Kossel" - GEF mode



Features appear at Bragg angle of **emitted** radiation

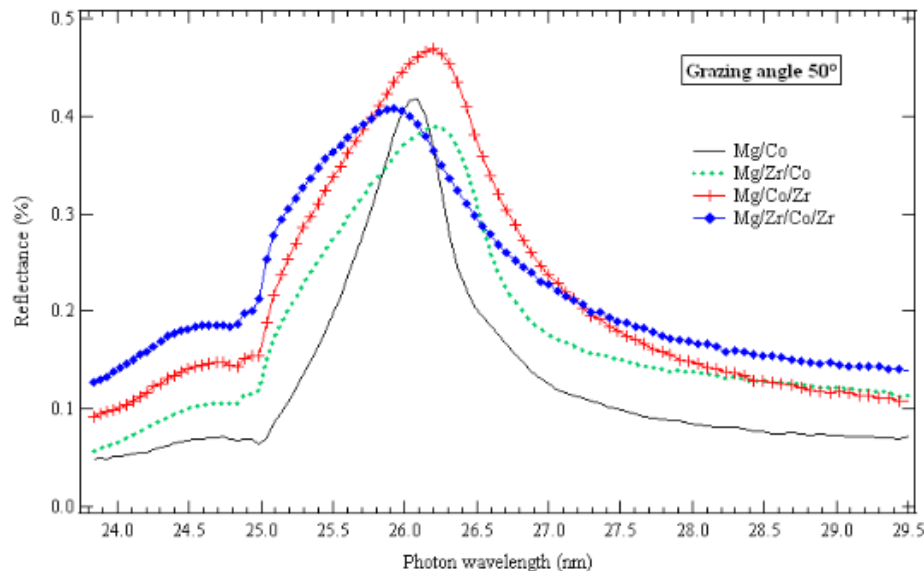


Do not move with energy of incident radiation

- Les ondes stationnaires (XSW)
- XSW – XRF: Co/Mg/Zr
- XSW – HAXPES: Pd/Y/B4C
- Kossel – XRF: Pd/Y/B4C

Introduction of Zr into Mg/Co stack

- Makes the stack stable upon annealing
- Improves the reflectivity (optimization on the optical path within the stack)

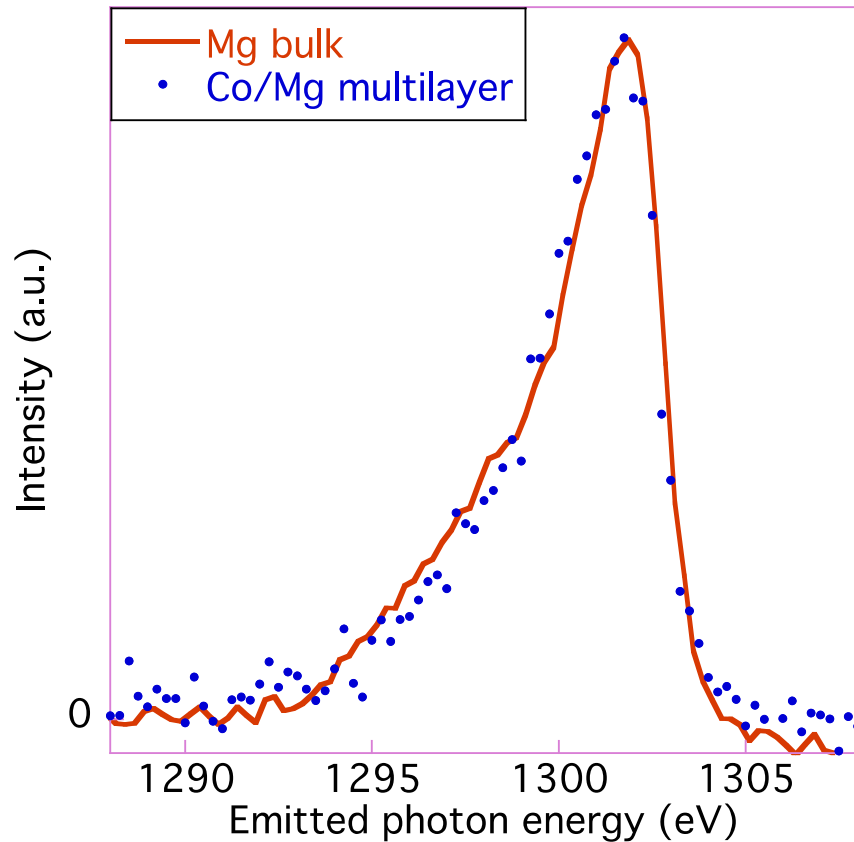


Reflectivity measurement
at the application wavelength
26 nm (50 eV)

Si substrate / [Mg (5.45nm) / Co (2.55nm) / Zr (1.5nm)]x30 / B4C (3.5nm)
Si substrate / [Mg (5.45nm)) / Zr (1.5nm) / Co (2.55nm)]x30 / B4C (3.5nm)

Two different orders of the layers

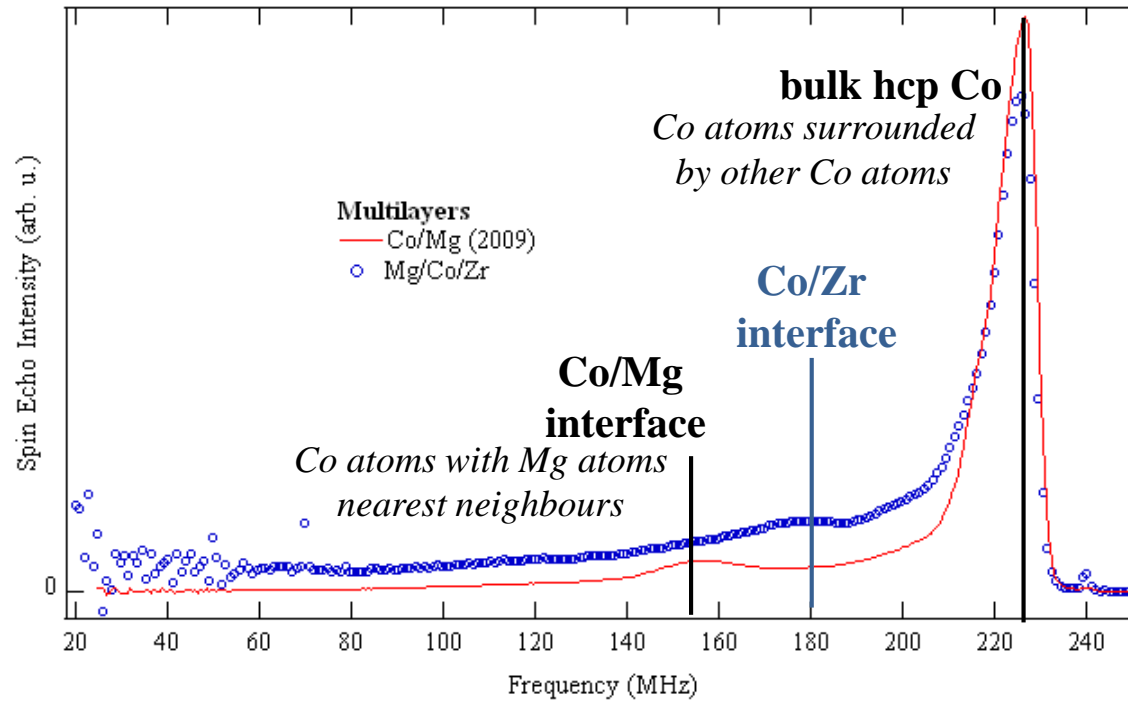
X-ray emission spectroscopy



- Mg atoms as in pure Mg
- No interaction between Mg and Co layers

NMR spectroscopy

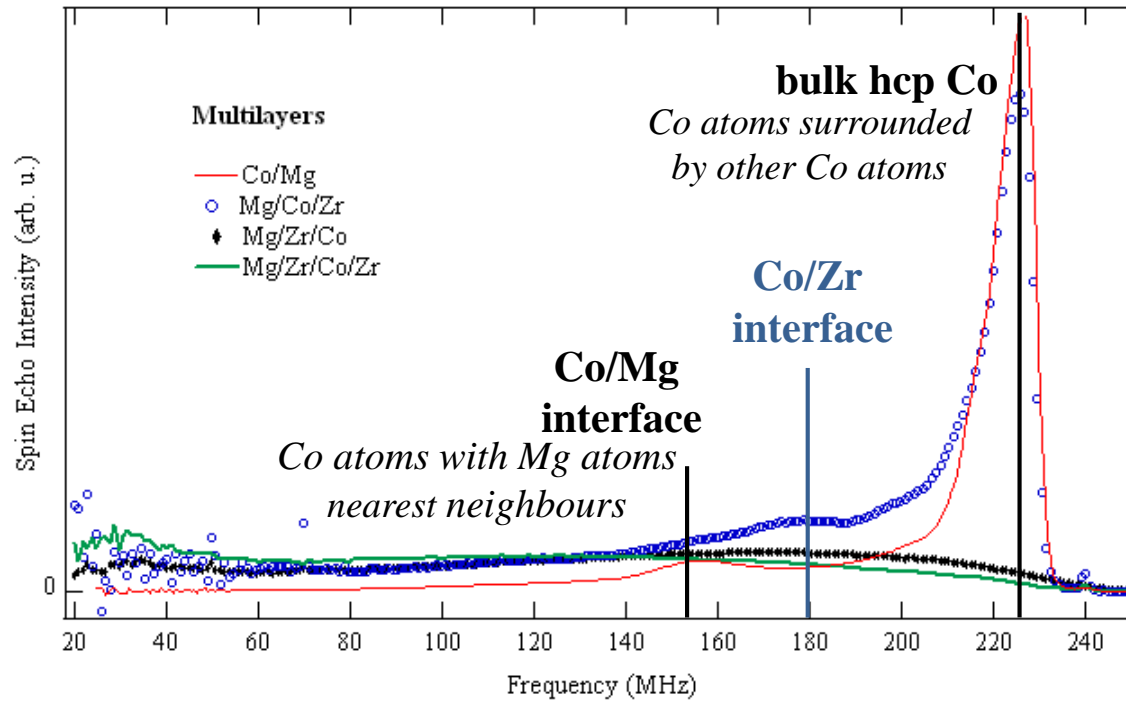
Probe of the nearest neighbour local structure around the Co atoms



Mg/Co and Mg/Co/Zr
well-defined layers and interfaces

NMR spectroscopy (3)

Probe of the nearest neighbour local structure around the Co atoms



Mg/Co and Mg/Co/Zr
well-defined layers and interfaces

Mg/Zr/Co and Mg/Zr/Co/Zr
strong intermixing between Co and Zr

Mg/Co and Mg/Co/Zr

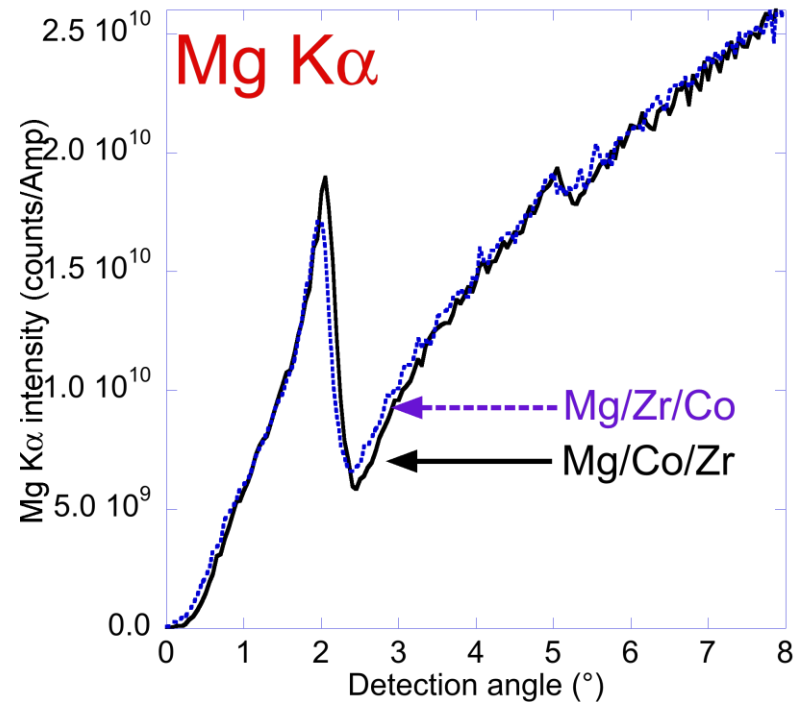
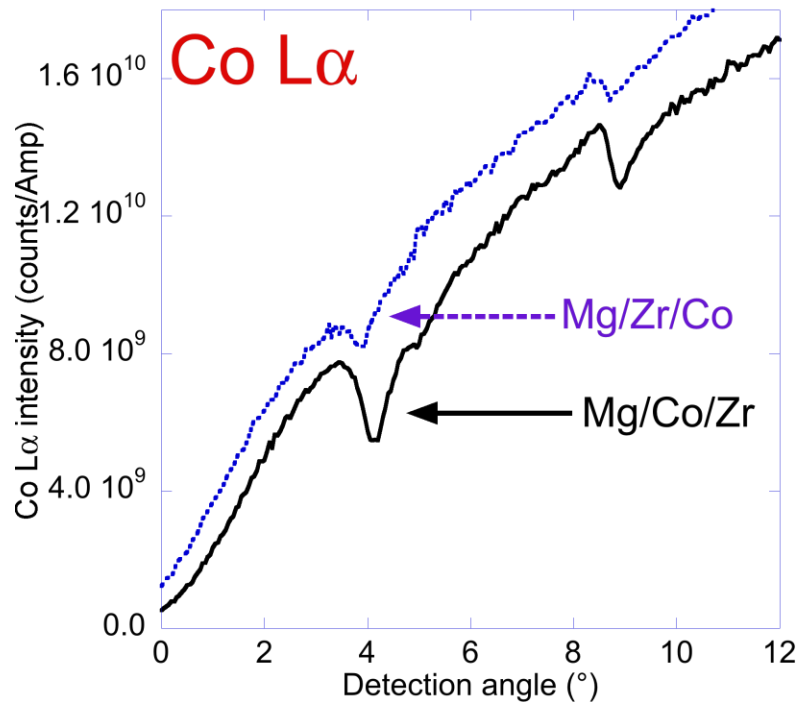
only geometrical roughness

Mg/Zr/Co and Mg/Zr/Co/Zr

reaction between Co and Zr

GE measurements – Mg-Co-Zr

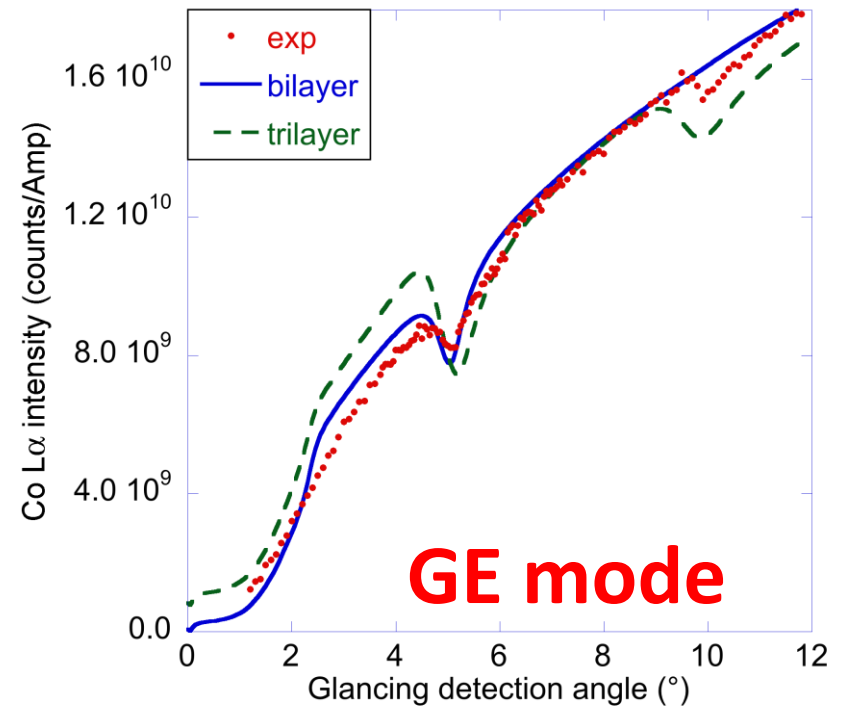
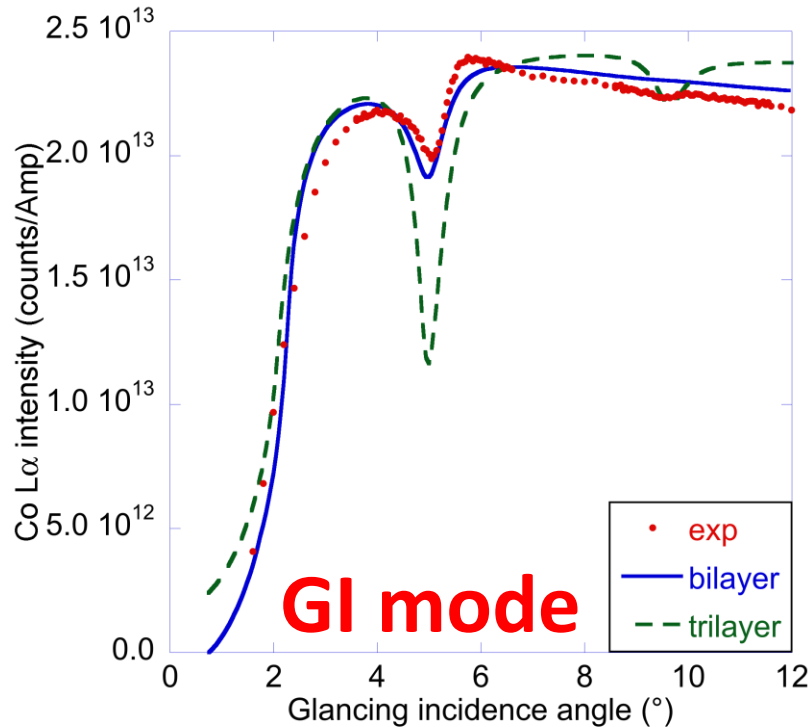
Different contrasts of the features for Co L emission depending on the sample



Same behavior in **GI mode**

Simulations – Mg-Co-Zr

Mg/Zr/Co – Co L emission



- Mg/Zr/Co **trilayer** described as Mg/Co₄Zr **bilayer**
- Mg/Co/Zr trilayer with nominal parameters

Mg-Co-Zr interfaces

From XRR, NMR, XES, XSW-XRF

- **Sharp Zr-on-Co interfaces** in Mg/Co/Zr
- **Mixing at Co-on-Zr interfaces** in Mg/Zr/Co

Surface free energy

- Co 2.0 J.m^{-2}
- Zr 1.6 J.m^{-2}



Asymmetric behavior of
Zr-on-Co and Co-on-Zr interfaces

- Les ondes stationnaires (XSW)
- XSW – XRF: Co/Mg/Zr
- XSW – HAXPES: Pd/Y/B4C
- Kossel – XRF: Pd/Y/B4C

Pd/Y based periodic multilayers

- **Problem: the original design has bad optical performance**

- X-ray reflectometry @ 8048 eV - Cu K radiation

Low reflectance, bad periodicity

- Severe interdiffusion between Pd and Y layers.

- **Solution: Derivative systems**
Interface engineering

- N₂ in the sputtering gas

0%

2%

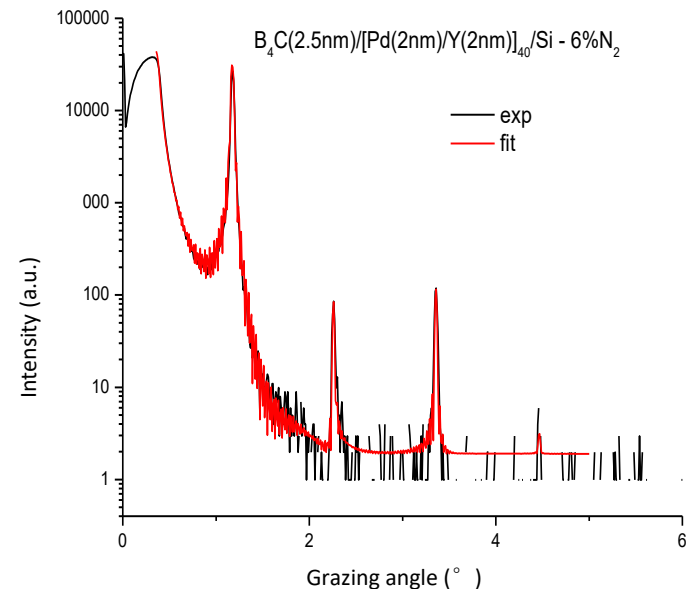
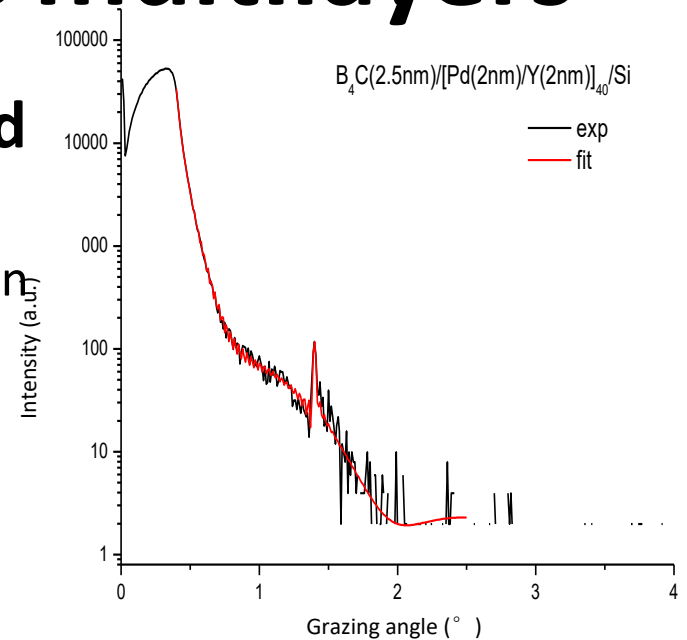
6%

- B₄C barrier layers at

Pd-on-Y interfaces

Y-on Pd interfaces

all interfaces

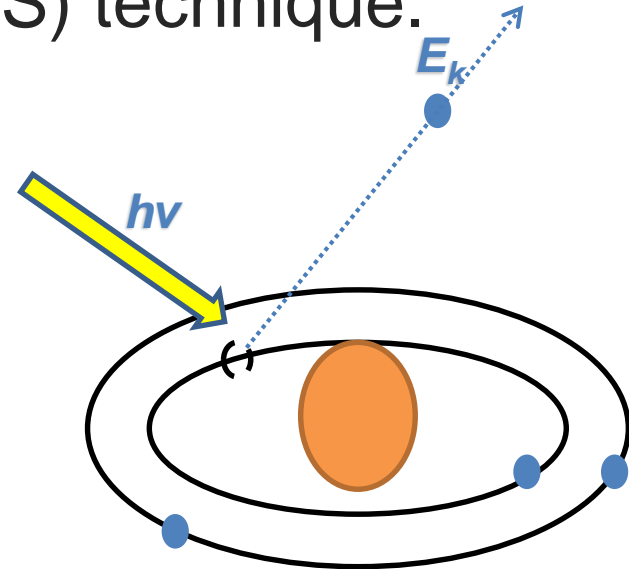


Methodology: HAXPES

- An extension of conventional X-ray Photoelectron Spectroscopy (XPS) technique.

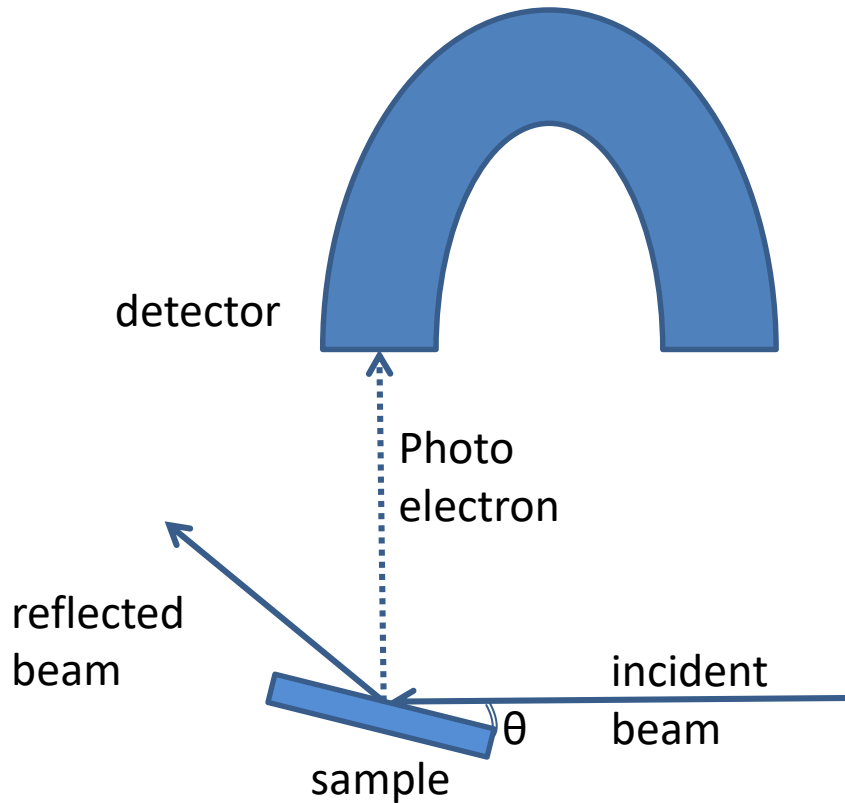
$$h\nu = E_b + \phi_{\text{spectrometer}} + E_k$$

- Higher incident photon energy.
 - Longer inelastic mean free path. Probed depth increases.
 - 10 keV => 22 nm (about 5-6 periods, bulk sensitive)
 - 3 keV => 9 nm (about 2 periods, surface sensitive)



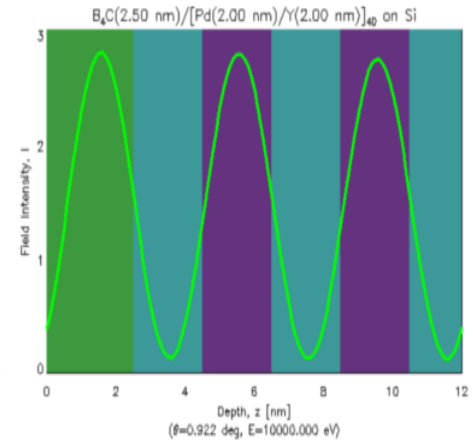
- GALAXIES beamline in SOLEIL Synchrotron.
 - High brilliance monochromatic x-ray source.
 - Small cross section due to high energy.

Methodology: combine HAXPES with XSW

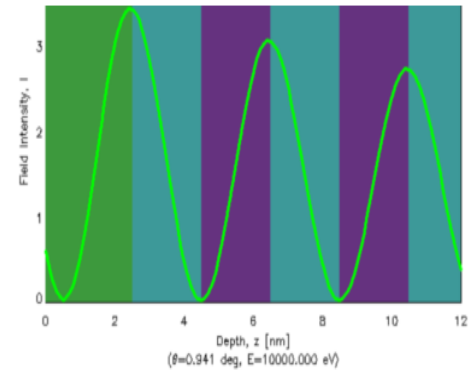


$$D = \frac{\lambda}{2 \sin \theta} = \frac{2\pi}{Q}$$

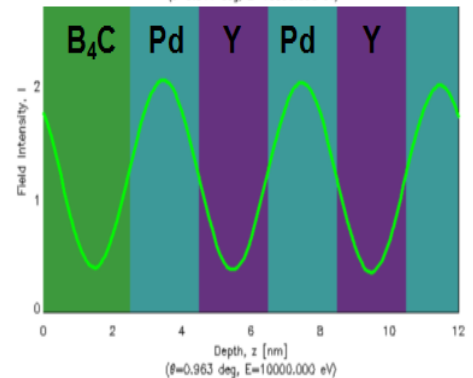
$\theta_i < \theta_{\text{Brag}}$
 \mathcal{E}



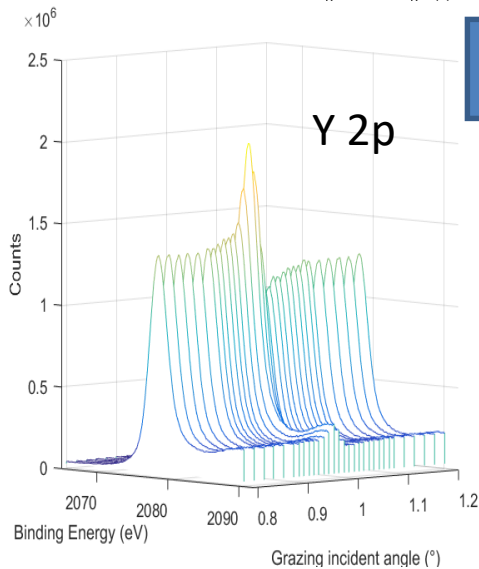
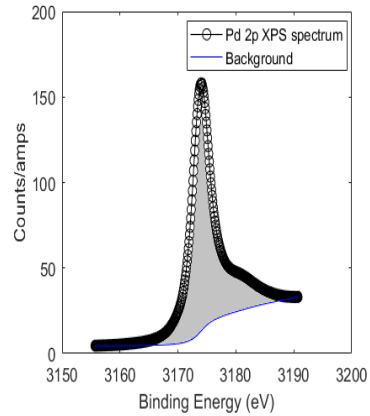
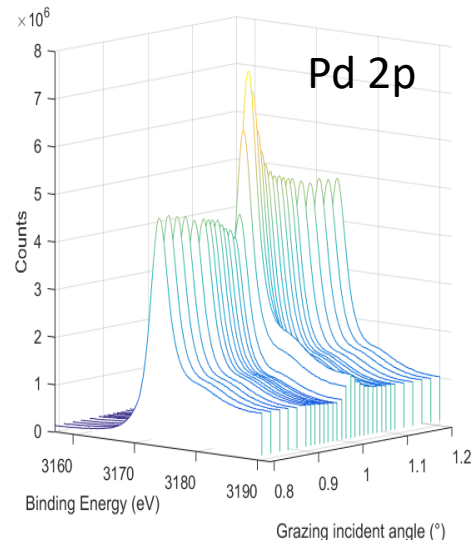
$\theta_i = \theta_{\text{Brag}}$
 \mathcal{E}



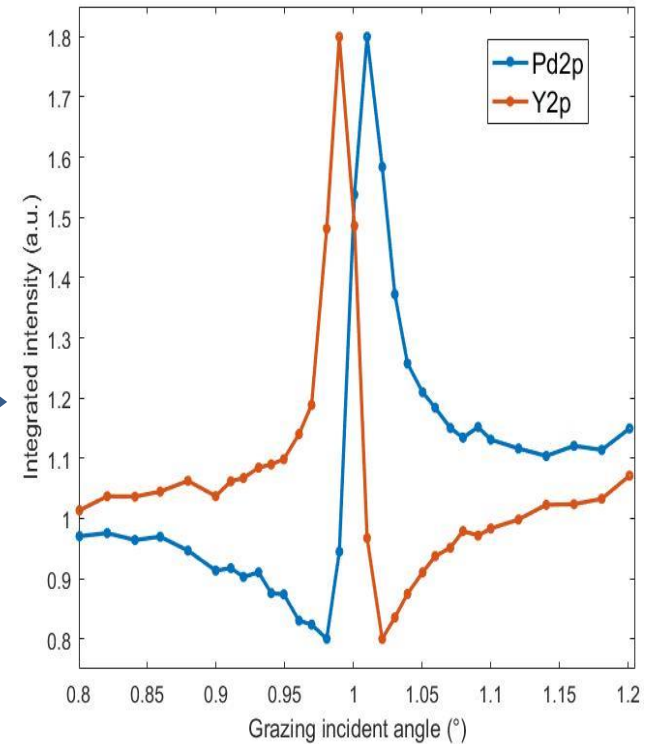
$\theta_i > \theta_{\text{Brag}}$
 \mathcal{E}



From HAXPES spectra to XSW curves



Integrate the peak considering a Shirley background.

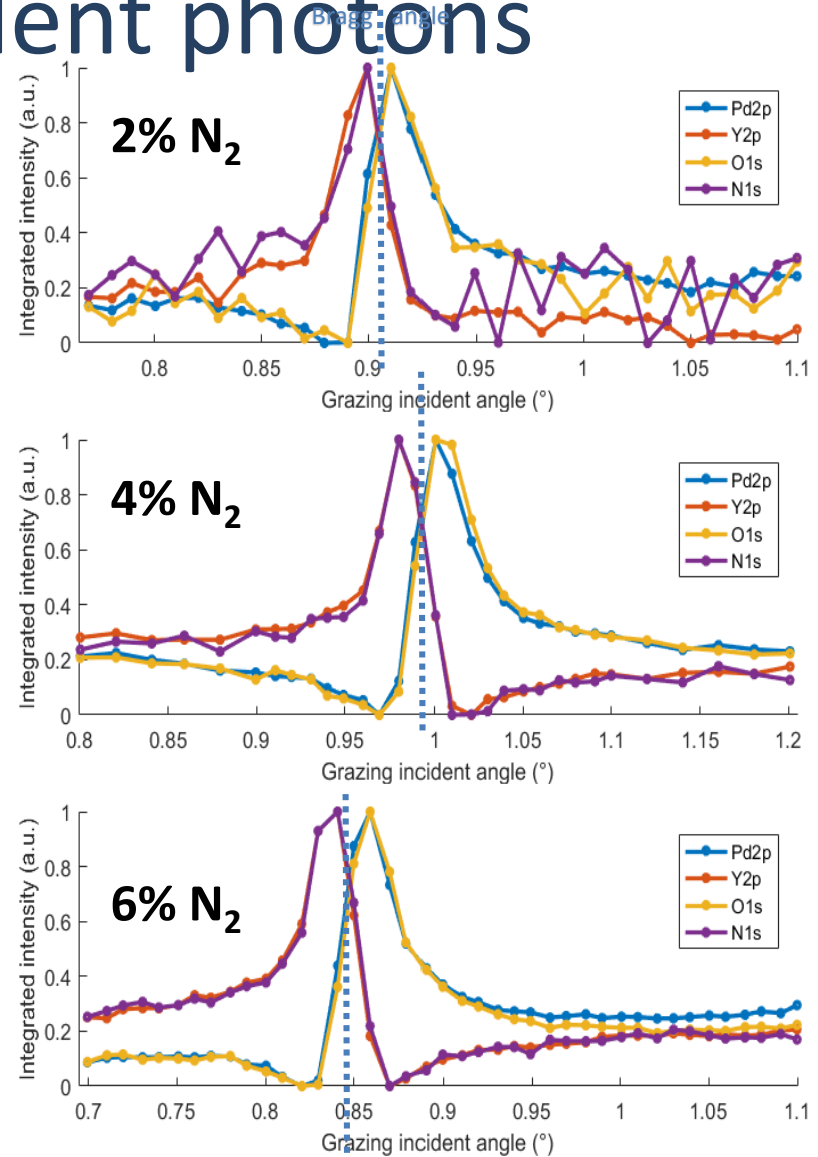


Result: XSW curves measured with 10 keV incident photons

- Bulk sensitive.
- XSW curves, extracted from photoemission spectra, of the Pd/Y multilayers prepared with 2, 4, 6 and 8% of N₂ respectively measured with a 10 keV incident photon energy.
- Elemental information in the stacks. Chemical selectivity.

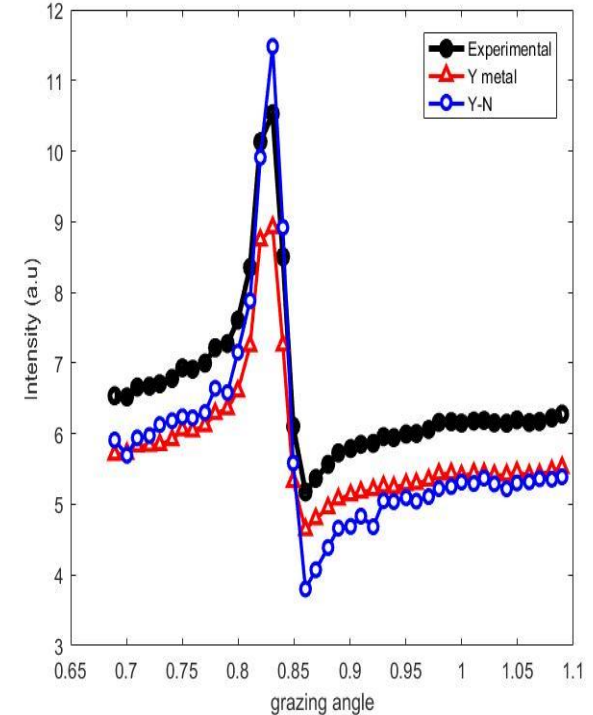
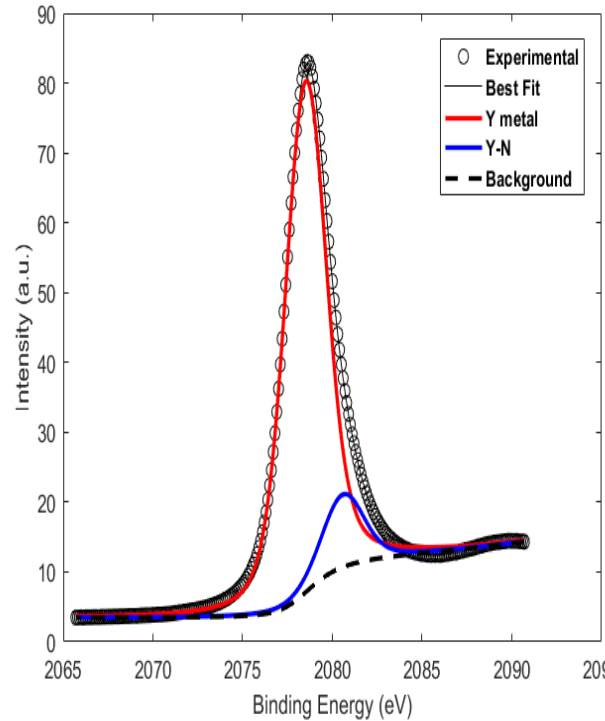
Pd & O

Y & N



Decomposition of Y 2p_{3/2} spectra

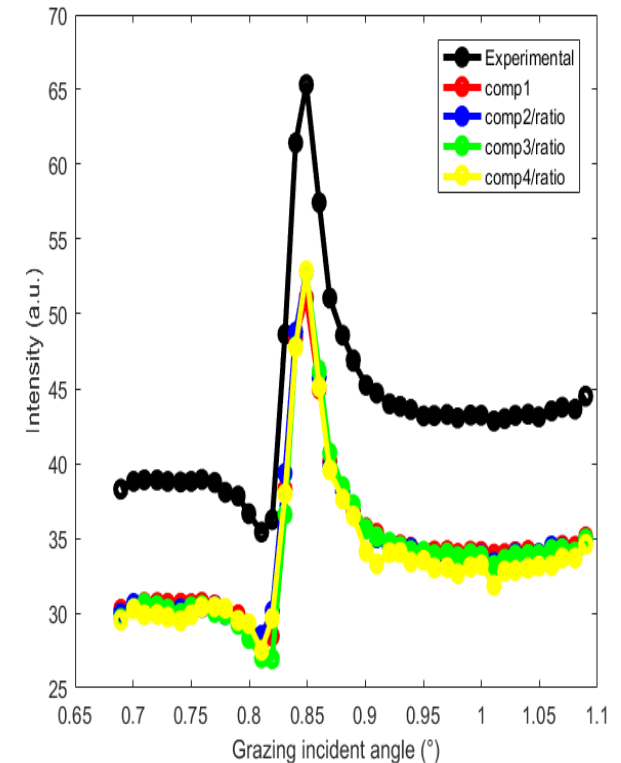
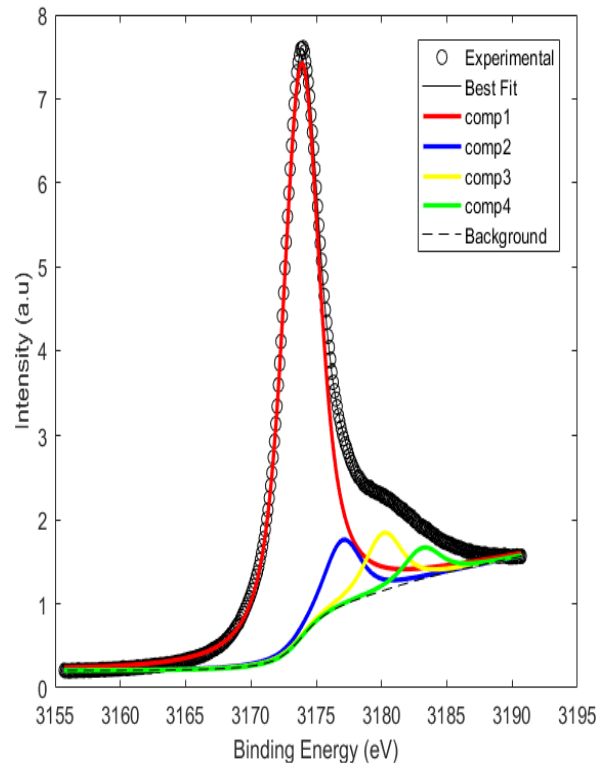
- Distribution of chemical states.
- 4-peak model was used to fit the spectra, only 2 peaks are necessary.
- Only **Y metal** and **YN** are presented in the Y layers.
- According to the XSW curve contrast, YN has less interdiffusion than Y.



Y 2p_{3/2} photoemission spectrum of the sample with 6% nitrogen in the sputtering gas (left), and the XSW curves corresponding to the sub-peaks (right).

Decomposition of Pd 2p_{3/2} spectra

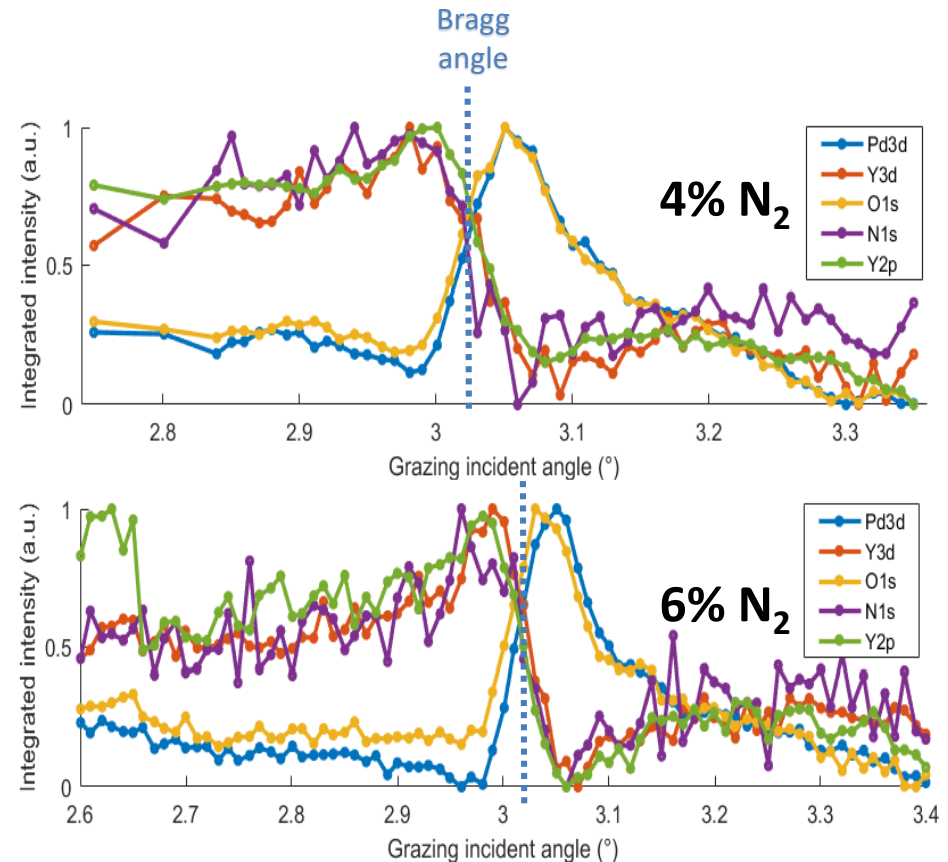
- **Distribution of different chemical states.**
- **XSW curves are normalized with the ratio compared to the main sub-peak.**
- **Multiple components have the same XSW curve.**
- **Homogeneous distribution of Pd and its oxides? No.**
- **Shake up satellite peaks**
- **=> oxide peak too close to metal peak.**



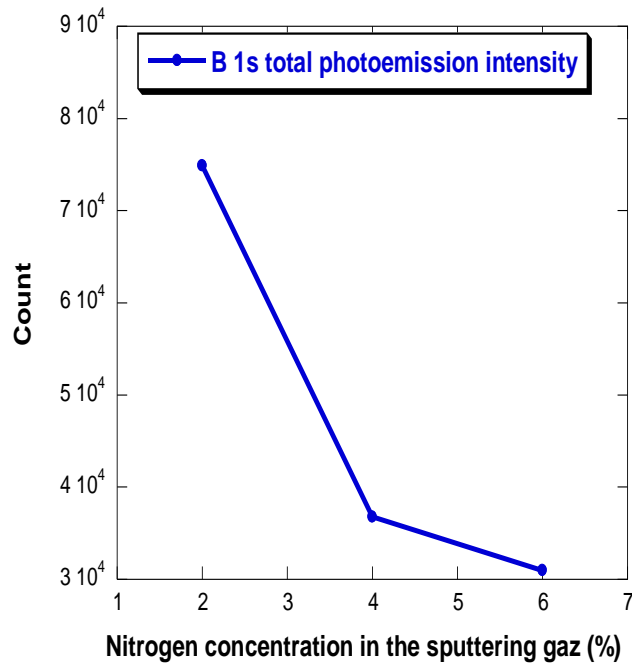
Pd 2p_{3/2} photoemission spectrum of the sample with 6% nitrogen in the sputtering gas (left), and the XSW curves corresponding to the sub-peaks (right).

Result: XSW curves measured with 3 keV incident photons

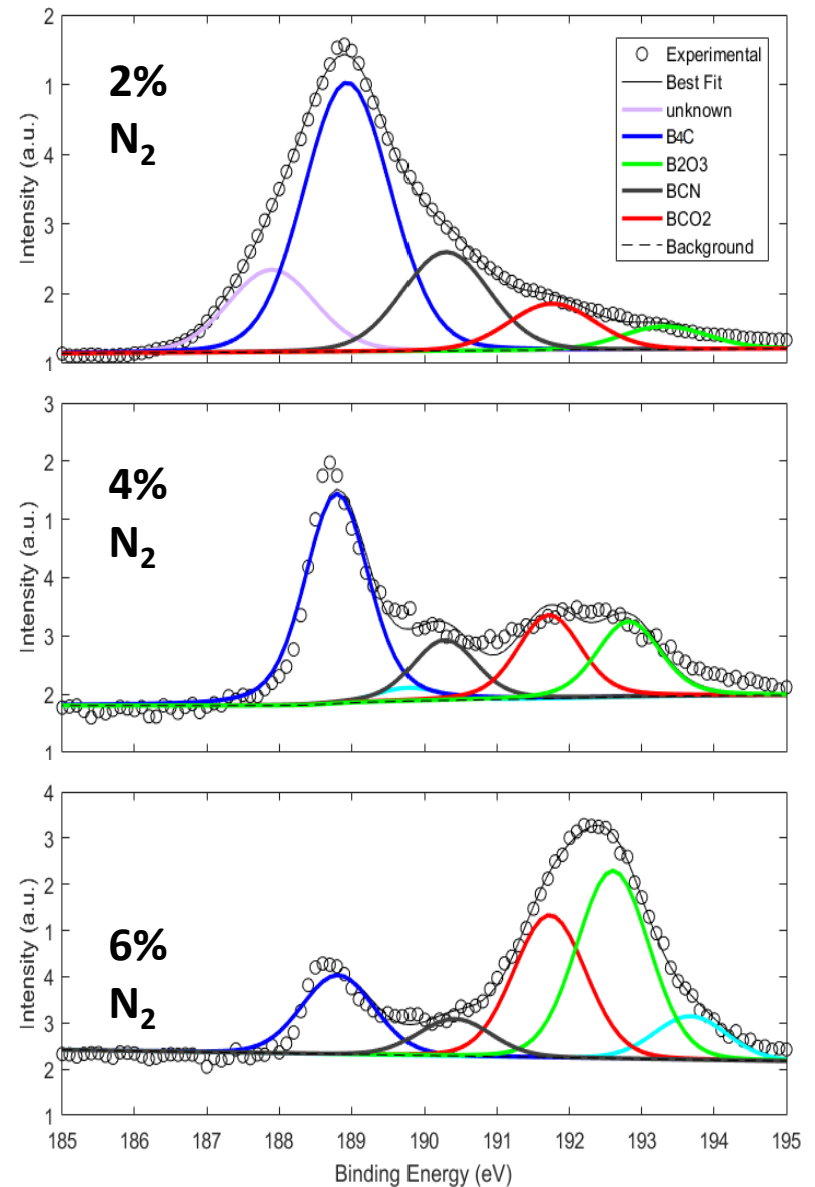
- Surface sensitive.
- XSW curves, extracted from photoemission spectra, of the Pd/Y multilayers prepared with 2, 4 and 6% of N₂ respectively measured with a 3 keV incident photon energy.
- 2% data unreliable due to instrumental problem.
- Elemental information in the stacks. Chemical selectivity.
Pd & O Y & N



Decomposition of B 1s spectra



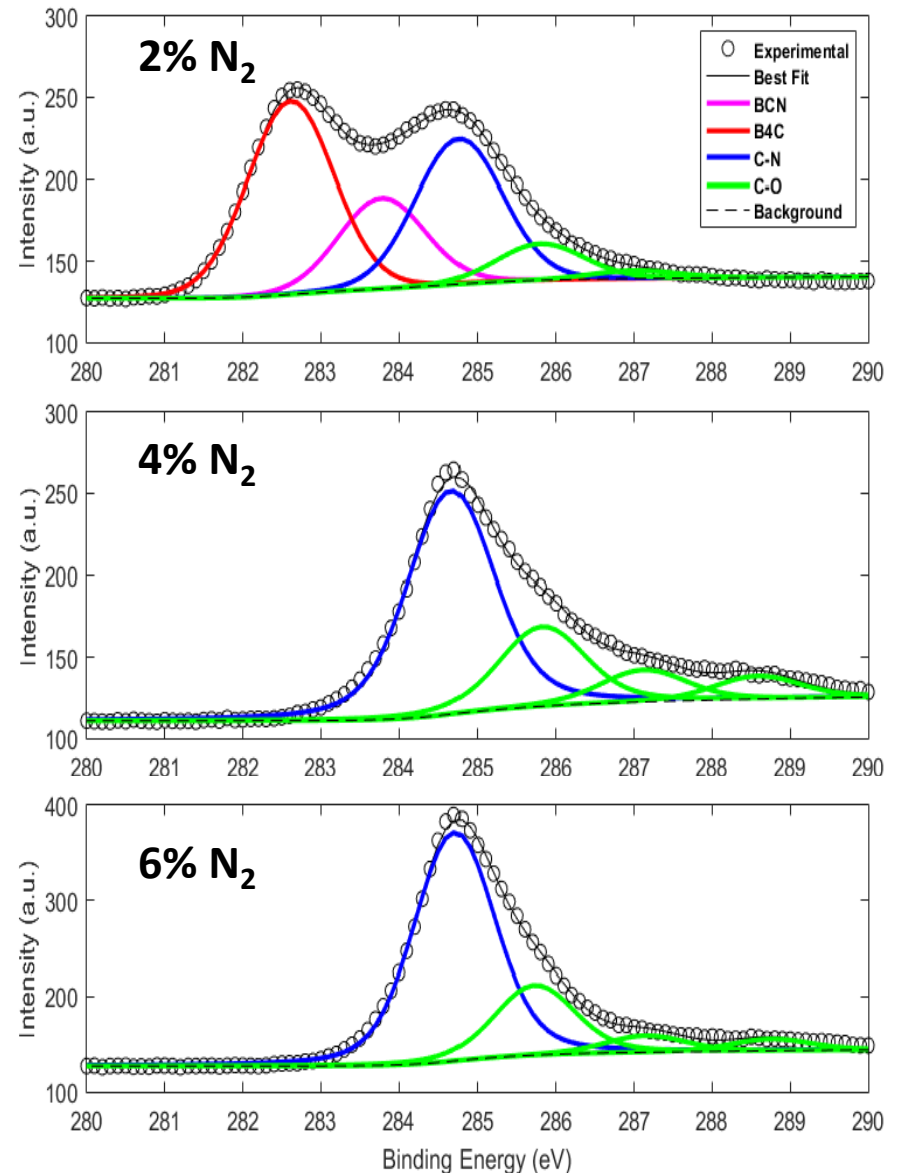
- B 1s total photoemission intensity decreases.
- B_4C component decreases.
- Cap material loss.



Decomposition of C 1s spectra

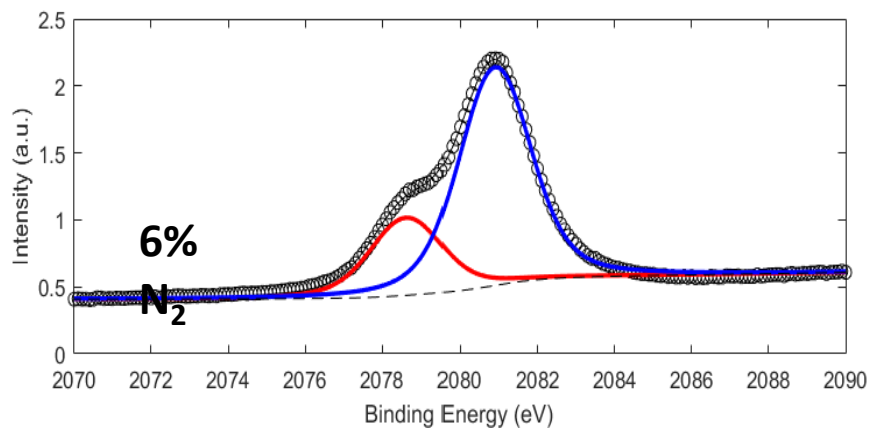
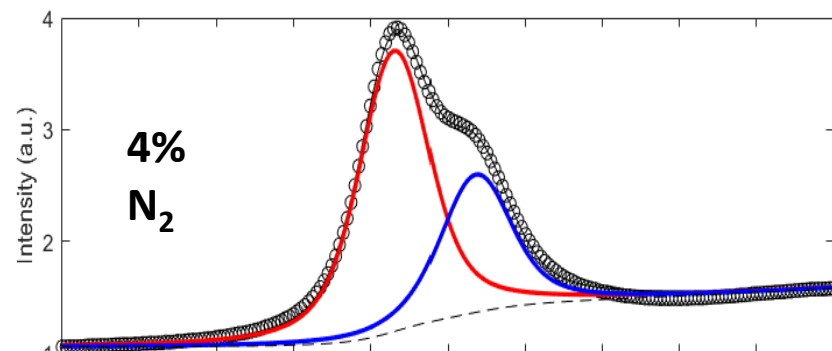
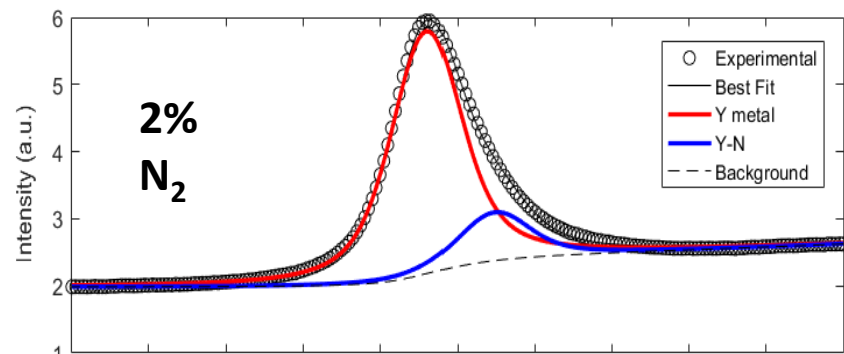
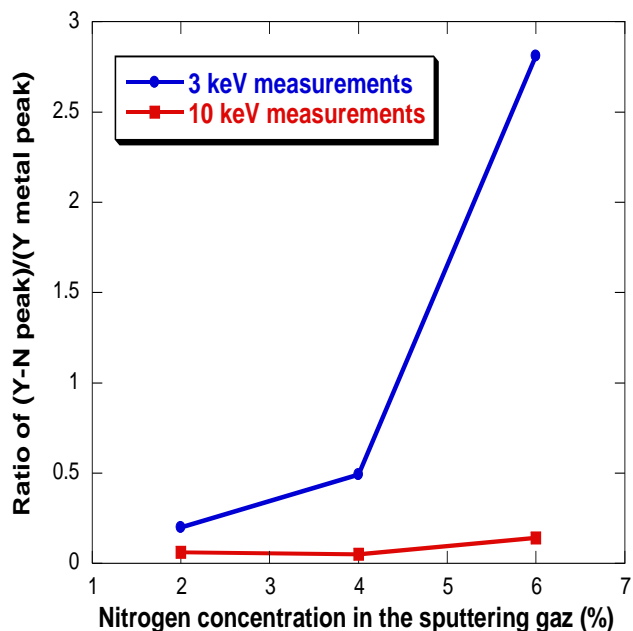
- B₄C component almost entirely disappears.
- Contamination becomes dominant.
- Cap material loss confirmed.
- Due to change of deposition rate.

Wang *et al.* "Nitridated Pd/B₄C multilayer mirrors for soft X-ray region: internal structure and aging effects," Opt. Express. 25, 7749 (2017).



Decomposition of Y 2p3/2 spectra

- Unexpected variation of YN concentration which only happens on the surface.



- The effect of X-ray standing wave enhancement is clearly observed.
- The information of elemental distribution is obtained indicating a chemical selectivity among the elements:
Y ♥ N Pd ♥ O
- Only Y metal and YN are presented in the Y layers. The formation of YN improves the optic performance of the multilayers.
- There is B₄C cap material loss when we add nitrogen in the sputtering gas due to the change of deposition rate.

- Les ondes stationnaires (XSW)
- XSW – XRF: Co/Mg/Zr
- XSW – HAXPES: Pd/Y/B4C
- Kossel – XRF: Pd/Y/B4C

Particle Induced X-ray Emission

- Particle Induced X-ray Emission (PIXE)

- Ionization: particle generated core hole
- X-ray emission (fluorescence)

- SAFIR platform in SU

- Système d'Analyse par Faisceaux d'Ions Rapides
(Analysis System using fast ions)
- Van de Graaff accelerator of positive ions
- 2 MeV proton beam, ionization of Pd L shell

- Advantages of protons

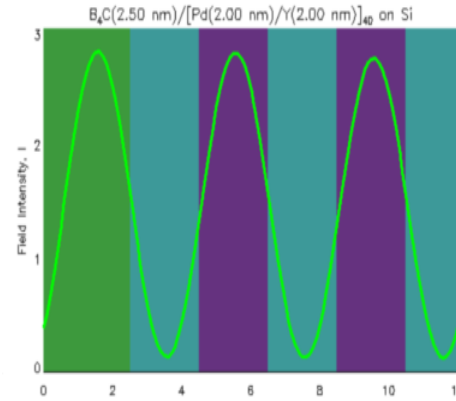
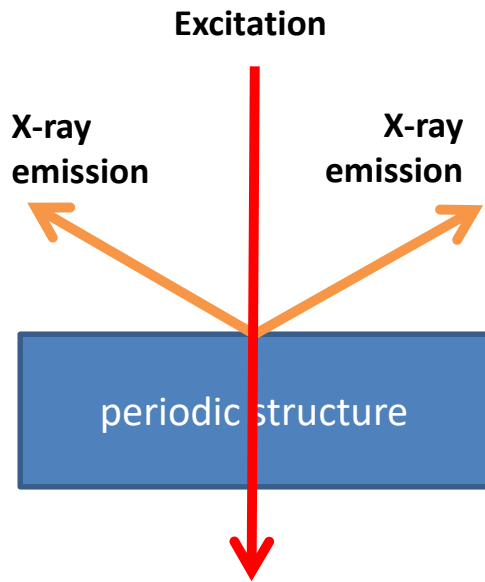
- Low scattering
- Low Bremsstrahlung
- Low energy loss (0.5% after penetrating the multilayer)
- Uniform ionization cross section



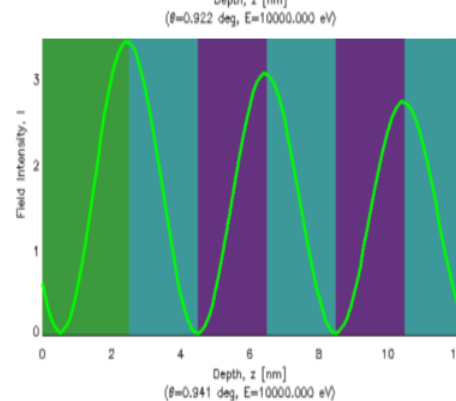
Van de Graaff accelerator in SAFIR

Combine PIXE with Kossel diffraction

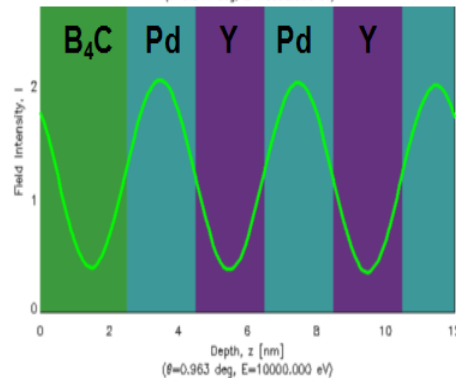
$$D = \frac{\lambda}{2 \sin \theta} = \frac{2\pi}{Q}$$



$\theta < \theta_{\text{Bragg}}$

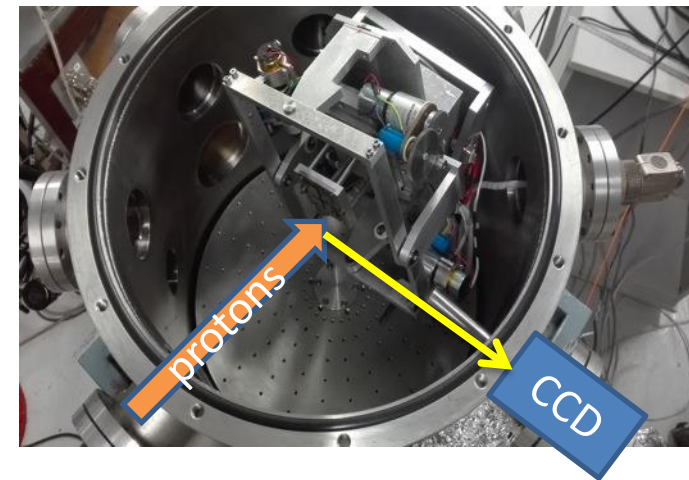
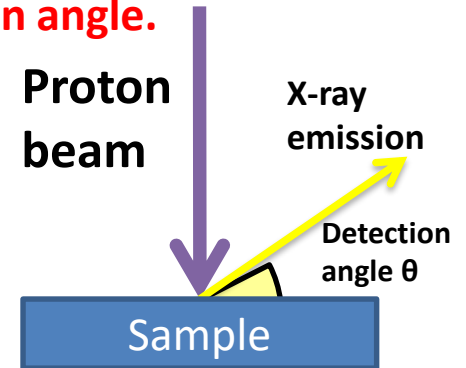


$\theta = \theta_{\text{Bragg}}$

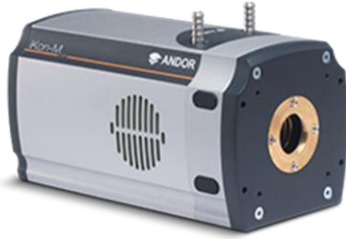


$\theta > \theta_{\text{Bragg}}$

Measurement of X-ray emission intensity as a function of the detection angle.



Energy dispersive CCD



Andor Ikon-M CCD

~150 eV resolution @5.9 keV

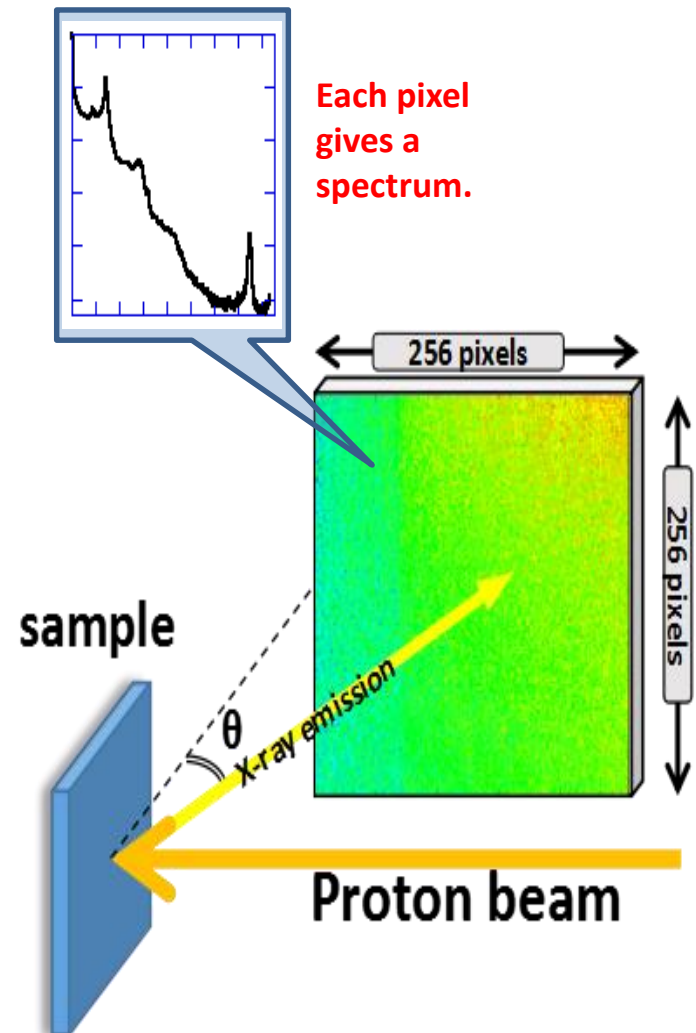
- **Advantage: spatially resolved**

- Measurement of X-ray emission intensity in a squared area of about 13 x 13 mm
- Native: 1024 x 1024 sensor array with 13 x 13 μm pixels
- Our selection: 256 x 256 pixels of 52 x 52 μm
- >>> **compromise of angular/energy resolution**

- **No need to scan the angle**

- We place a 200 μm beryllium film in front of the camera to filter the scattered protons. **Protection of the camera**
- Acquisition time significantly reduced compared to SDD

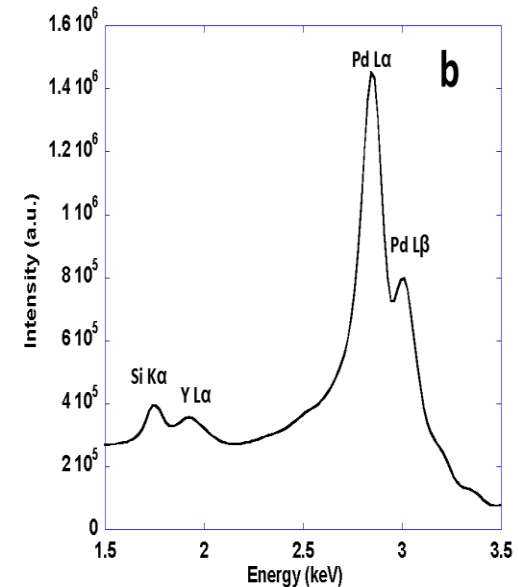
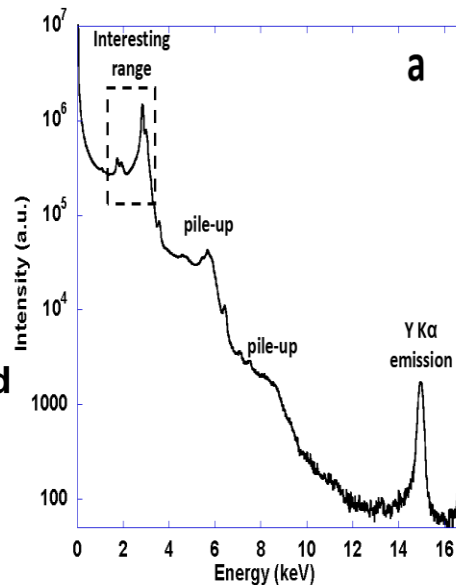
Days to 2 hours >>>potential of *in situ* measurements (annealing test, oxidation test)



X-ray emission spectrum

- $B_4C(2.5 \text{ nm})/[Pd(2 \text{ nm})/B_4C(2 \text{ nm})/Y(2 \text{ nm})]_{x40}/Si$
- Energy resolution is about 150 eV at 5.9 keV (Mn $K\alpha$).
- Pd $L\alpha$ $L\beta$, Y $L\alpha$ $K\alpha$, Si $K\alpha$ can be observed
- Pile up effect due to multiple photons detection
- Energy calibration of the spectrum is carried out with
Pd $L\alpha$ (2.838 keV) and Y $K\alpha$ (14.958 keV)

- Y $K\alpha$ has too low intensity.
- Y $L\alpha$, Si $K\alpha$ are in the low efficiency part of the X-ray camera.
- Pd $L\beta$ does not bring additional information
- **We measure Pd $L\alpha$ emission**

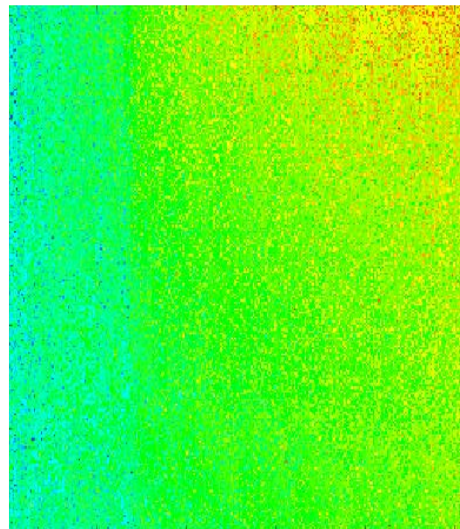
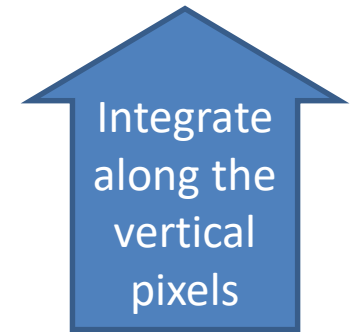
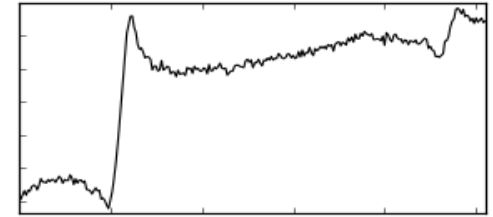


X-ray spectrum of Pd (2nm) / B_4C (2nm) / Y (2nm) periodic tri-tilayer:

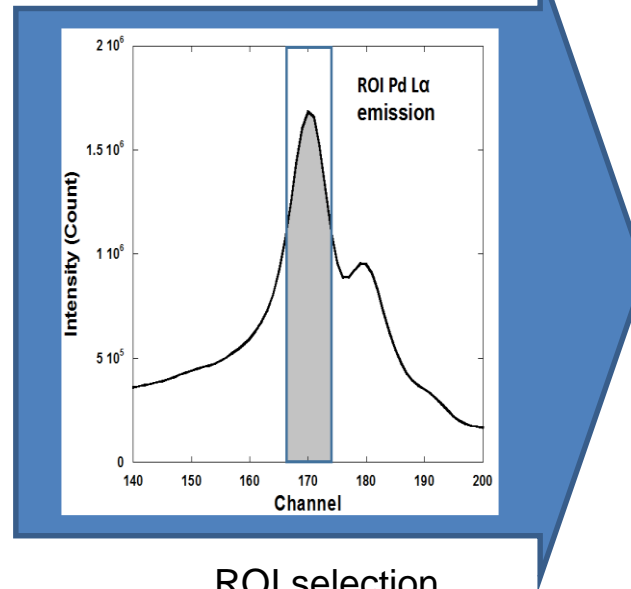
- a) overview (log scale)
- b) zoomed range of interest (linear scale).

Kossel curves

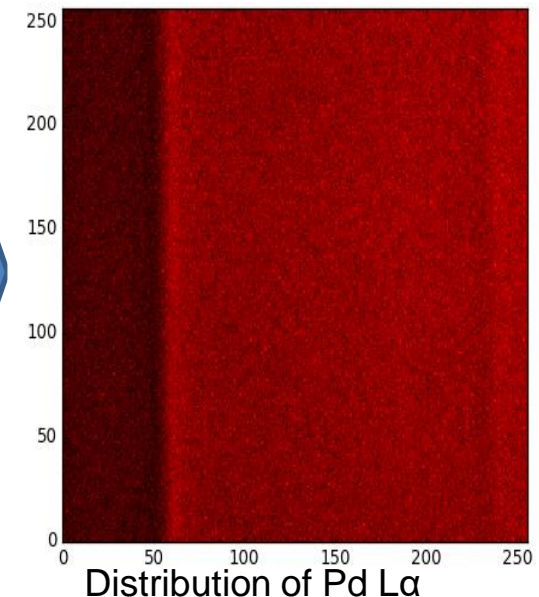
- The original image obtained by X-ray color camera contains the intensity of emitted photons of all energies.
- Kossel curve: the angular distribution of the characteristic X-ray emission.
- To get the Kossel curve of Pd L α emission, we need 3 steps:
 1. Select region of interest (ROI) on the spectrum.
 2. “Filter” the original image by applying ROI.
 3. Integrate the “filtered” image along the vertical pixels.



Distribution of X-ray emission



ROI selection



Distribution of Pd L α

Calibration of detection angle

- Pixel of the detector - grazing exit angle

- 4-layer sample:

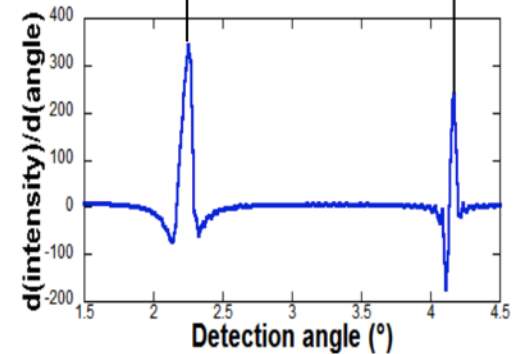
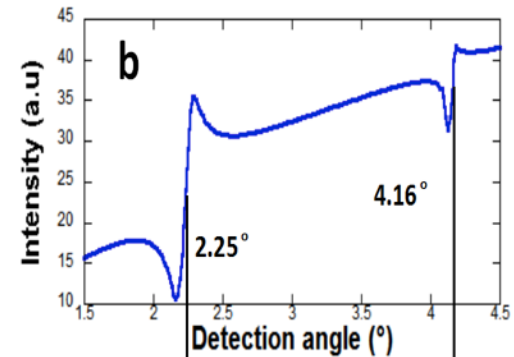
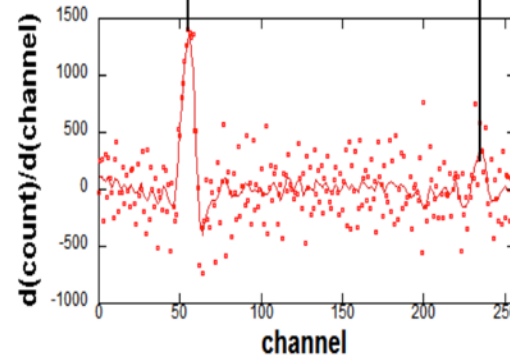
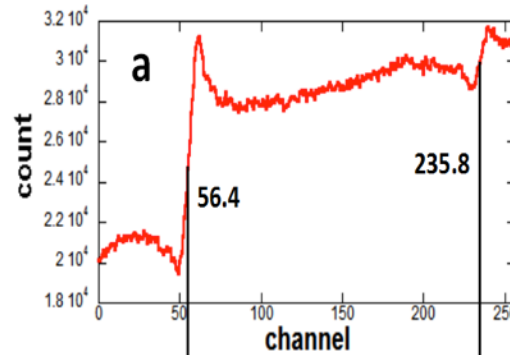
$B_4C(2.5 \text{ nm})/[B_4C(1 \text{ nm})/Pd(2 \text{ nm})/B_4C(1 \text{ nm})/Y(2 \text{ nm})]_{x40}/Si$

- 1st and 2nd order of Kossel oscillation

a) experimental curve in channel (pixel)

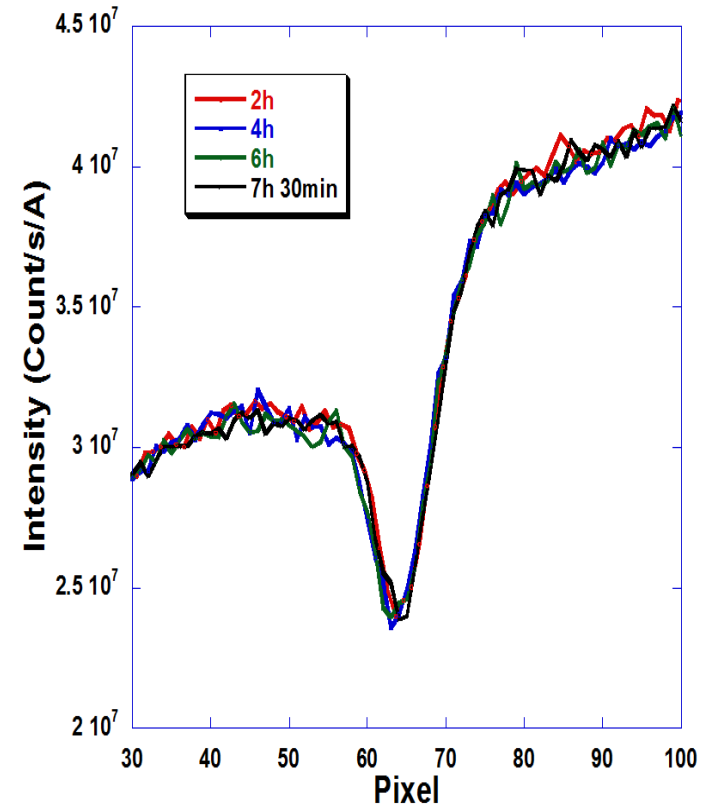
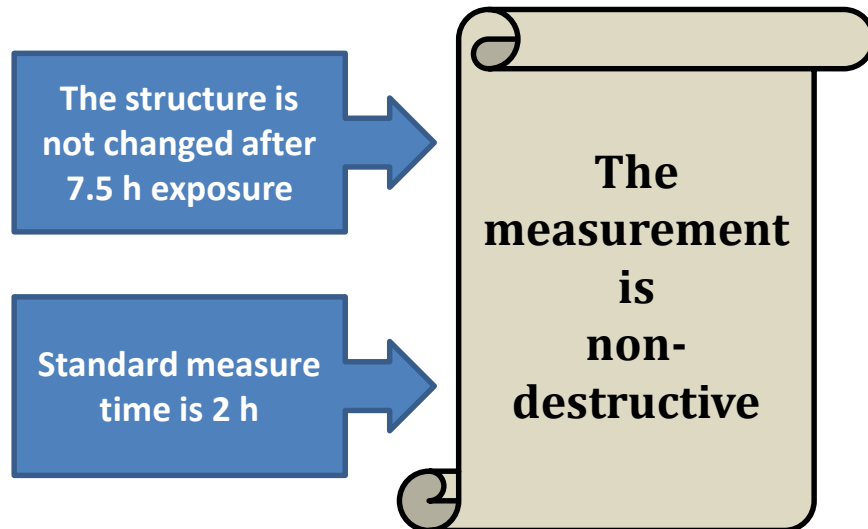
b) simulated curve in angle (degree)

- Precise values obtained from the derivatives of the curves



Non-destructive test

- $B_4C(2.5 \text{ nm})/[Pd(2 \text{ nm})/B_4C(2 \text{ nm})/Y(2 \text{ nm})]_{x40}/Si$
- Exposure under proton beam for 7.5 hours
- Kossel curve maintains its shape

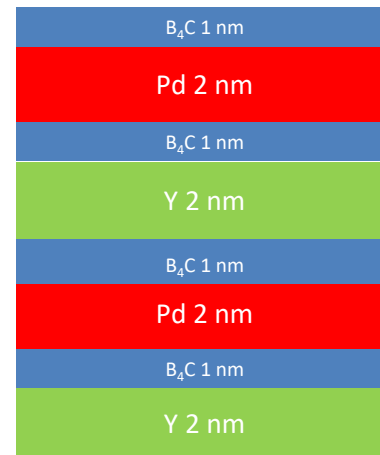
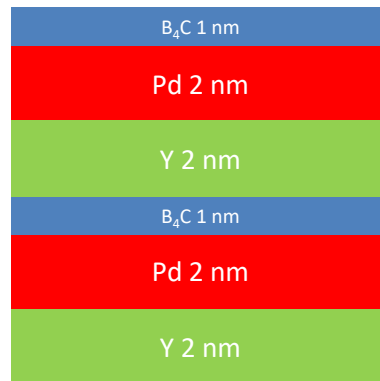
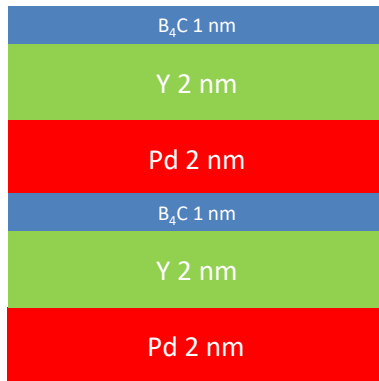


First observations of multilayer structures

It is known that Pd and Y intermix easily during magnetron sputtering, and thus need stabilising

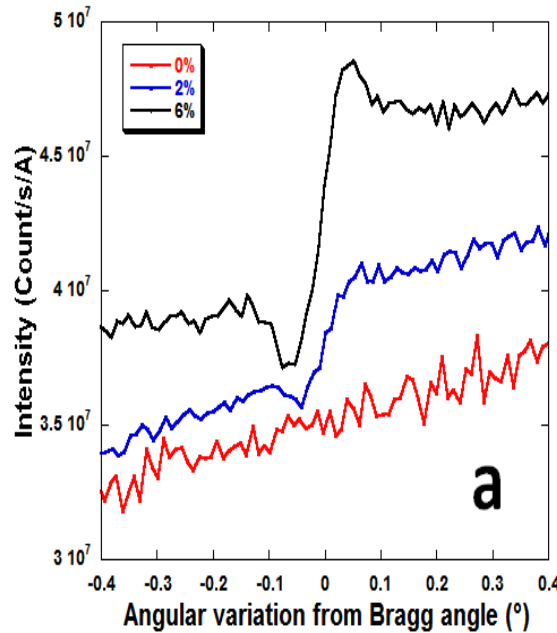
Interface engineering:

- Introduce N_2 into the plasma during growth – 0%, 2%, 6%
- Use 1 nm B_4C buffer layers

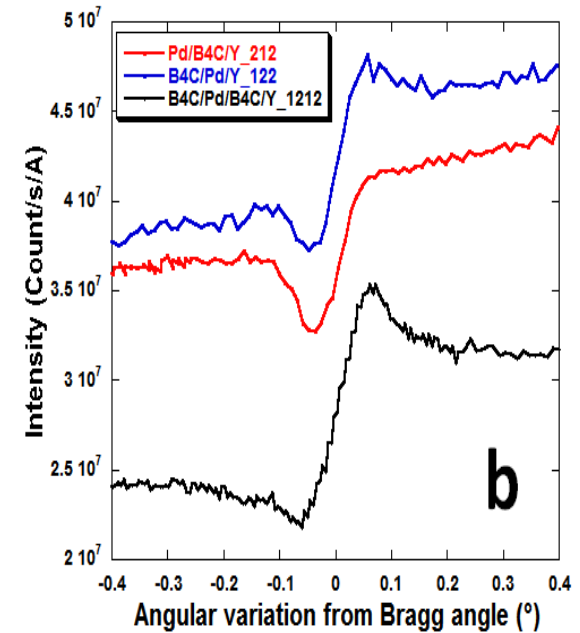


Kossel curves of Pd La emission

- 2-hour acquisition time. Curve statistics can be further improved by increasing the acquisition time.
- Angles are adjusted to the Bragg angle, which is in most cases located in the center of the Kossel oscillation.
- The periodicity of the originally designed Pd/Y multilayer is totally compromised.
- Nitrogen reduces the interdiffusion.
- Kossel features can be distinguished for samples with different B₄C barrier layers. **Structural sensitivity.**



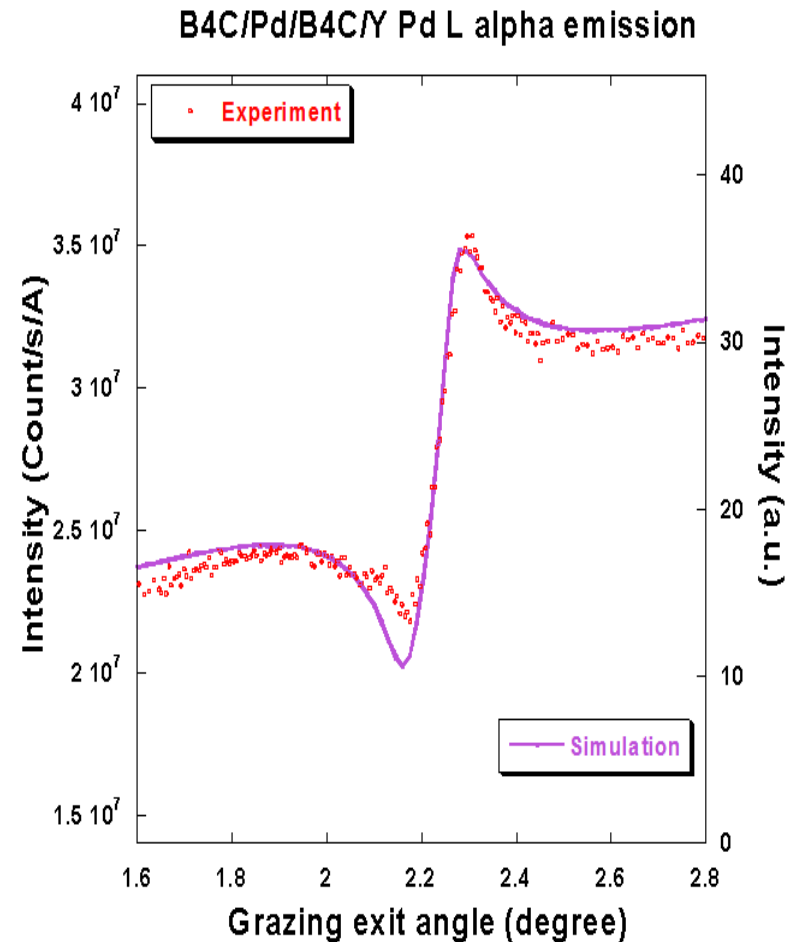
Kossel curves of the series of samples:
a) Deposited with nitrogen in the sputtering gas.



Kossel curves of the series of samples:
b) With B₄C barrier layers. The notation gives multilayer structure and layer thickness respectively.

Simulation

- Simulation of the PIXE-Kossel curve
- Code for XRF-Kossel curve
- Approach
- Uniform ionization
- Still not perfect due to background
- Improvement needed



CONCLUSION

LCPMR – SU

Karine LE GUEN

Jean-Michel ANDRE

Meiyi WU

Jiaping ZHANG

Vita ILAKOVAC



INSP – SU

Ian Vickridge

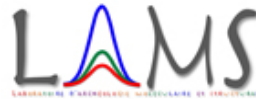
Didier Schmaus

Emrick Briand



LAMS – SU

Philippe Walter



LPCMS Strasbourg

C. Mény



Synchrotrons

A. Giglia (Elettra, IOM)

J.-P. Rueff (SOLEIL, LCPMR)



Institut d'Optique - Palaiseau

Franck Delmotte

Sébastien de Rossi

Françoise Bridou

Institut d'Optique – Tongji

Zhanshan Wang

Qiushui Huang